

Design, Synthesis, Dynamic Docking, Biochemical Characterization, and *in Vivo* Pharmacokinetics Studies of Novel Topoisomerase II Poisons with Promising Antiproliferative Activity

Jose M. Arencibia,[§] Nicoletta Brindani,[§] Sebastian Franco-Ulloa, Michela Nigro, Jissy Akkarapattiakal Kuriappan, Giuliana Ottonello, Sine Mandrup Bertozzi, Maria Summa, Stefania Giroto, Rosalia Bertorelli, Andrea Armirotti, and Marco De Vivo*



Cite This: <https://dx.doi.org/10.1021/acs.jmedchem.9b01760>



Read Online

ACCESS |



Metrics & More

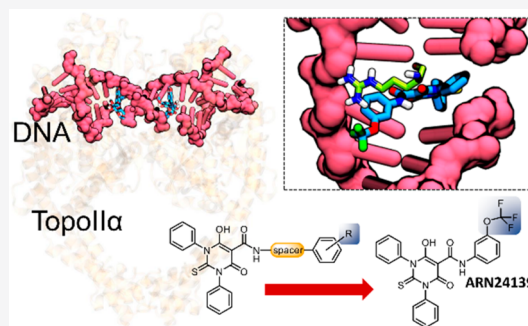


Article Recommendations



Supporting Information

ABSTRACT: We previously reported a first set of hybrid topoisomerase II (topoII) poisons whose chemical core merges key pharmacophoric elements of etoposide and merbarone, which are two well-known topoII blockers. Here, we report on the expansion of this hybrid molecular scaffold and present 16 more hybrid derivatives that have been designed, synthesized, and characterized for their ability to block topoII and for their overall drug-like profile. Some of these compounds act as topoII poison and exhibit good solubility, metabolic (microsomal) stability, and promising cytotoxicity in three cancer cell lines (DU145, HeLa, A549). Compound 3f (ARN24139) is the most promising drug-like candidate, with a good pharmacokinetics profile *in vivo*. Our results indicate that this hybrid new chemical class of topoII poisons deserves further exploration and that 3f is a favorable lead candidate as a topoII poison, meriting future studies to test its efficacy in *in vivo* tumor models.



INTRODUCTION

Human topoisomerase II (topoII) enzymes are a validated target to treat cancer because of their role in modifying the topology of entangled DNA strands during vital cellular processes like replication and transcription.^{1–4} Several topoII anticancer inhibitors are clinically available. One example is etoposide, which is used to treat a variety of cancers, including leukemia and ovarian cancer.^{5–9} However, drug resistance and the possibility of severe side effects of topoII-targeting drugs mean that researchers continue to seek novel safer topoII inhibitors.^{6,10–17}

Small molecules targeting topoII are classified as either topoII poisons or topoII catalytic inhibitors.^{18–20} These two classes of topoII blockers differ in their mode of action. TopoII poisons act by trapping the covalent topoII/DNA cleavage complex, which is formed during the catalytic cycle required for DNA topology modification. A covalent and stable topoII/DNA cleavage complex eventually leads to the accumulation of double-strand breaks, causing cell death.^{1,12,13,18,21–23} The chemotherapy drug etoposide (Figure 1) acts via this mechanism, although its pharmacological action can lead to severe side effects.^{24–26} Additional examples of anticancer drugs^{27–30} that act as a topoII poison are doxorubicin, mitoxantrone, salvicine, and teniposide. These drugs are frontline therapies for a wide range of solid and hematological malignancies.^{31–33}

TopoII catalytic inhibitors act differently than poisons and do not generate an accumulation of topoII/DNA cleavage complex. Instead, topoII catalytic inhibitors act, for example, by inhibiting DNA binding and/or by blocking the ATP-binding site in topoII, thus preventing ATP hydrolysis, which is needed for topoII function.¹⁹ One notable example is merbarone, which was one of the first and most promising topoII inhibitors (Figure 1).^{34–37} Merbarone is a thiobarbituric derivative (6-hydroxy-4-oxo-N-phenyl-2-thioxo-1H-pyrimidine-5-carboxamide) that blocks topoII catalysis and inhibits proliferation of several cancer cell lines.³⁵ Notably, merbarone underwent clinical trials as a chemotherapy drug.^{34,36} These trials failed because merbarone displayed nephrotoxicity issues and did not generate the expected efficacy.³⁸

Recently, we used a pharmacophore hybridization strategy to realize a first set of new topoII poisons.³⁹ They were rationally designed by combining key pharmacophoric elements of etoposide and merbarone to generate a new etoposide-merbarone hybrid active scaffold.^{39,40} In particular,

Received: October 30, 2019

Published: March 20, 2020

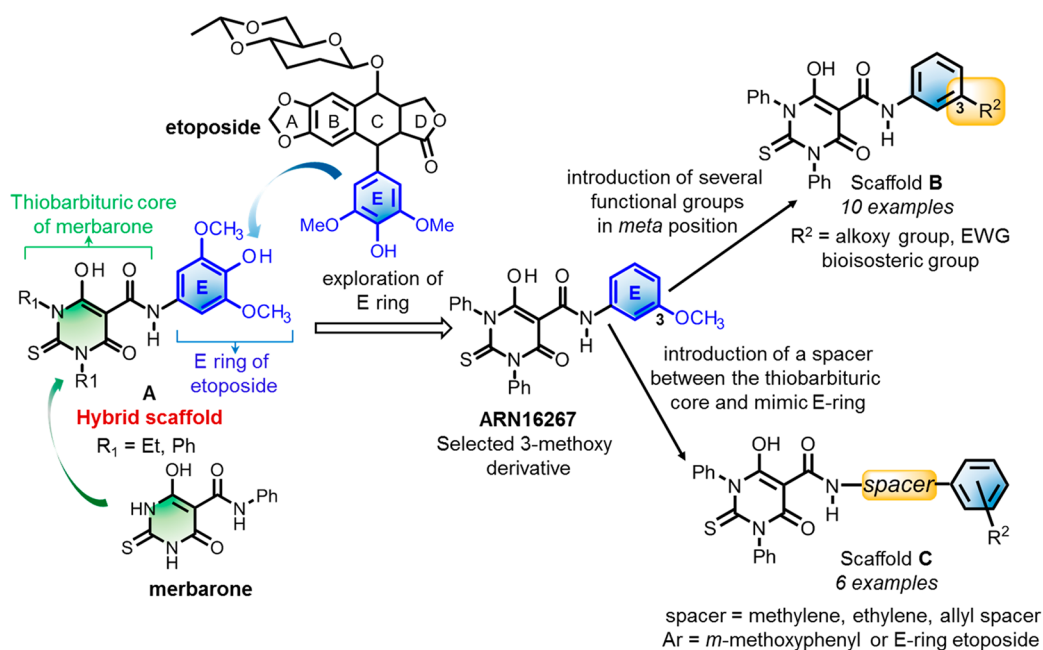
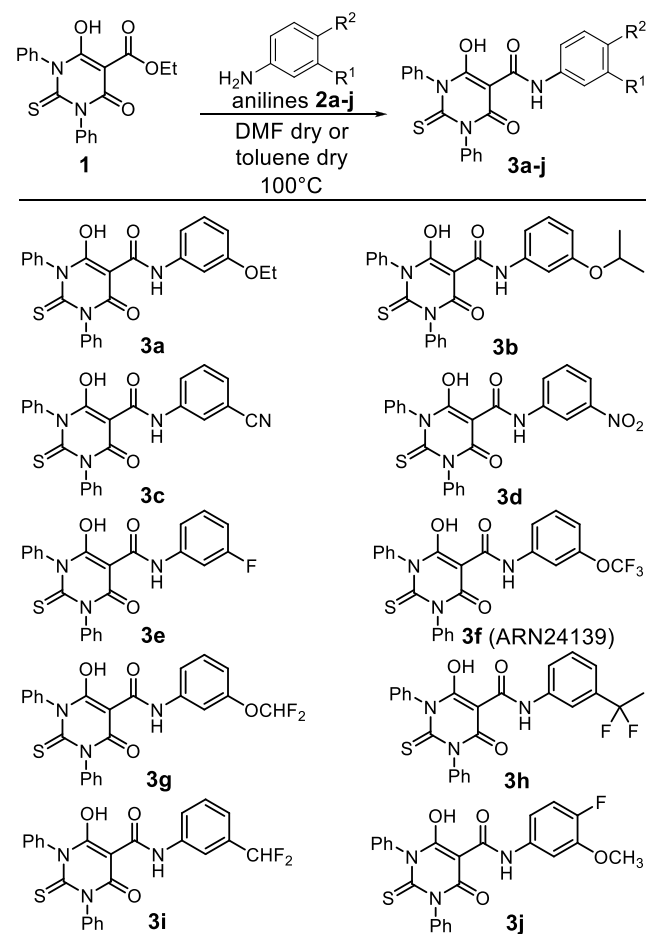


Figure 1. Hybrid topoII poison with the scaffold A (left) was explored to discover ARN16267 as a potent topoII blocker.³⁹ Here, the hybrid scaffold A was expanded to generate structures of type B (upper right), with several functional groups introduced in the *meta* position. Structures of type C (lower right) were generated by introducing a spacer between the thiobarbituric core and the mimic E-ring.

we designed, synthesized, and characterized a first set of compounds that feature the thiobarbituric core of merbarone linked via an amide bond to the E-ring of etoposide (type A structure, Figure 1). This design generated new *N,N'*-diphenyl derivatives that potentially block human topoII.³⁹ In addition, our SAR studies clarified the effect of ethyl and phenyl substitutions at each nitrogen of the thiourea moiety, as well as the influence of the number and/or position of hydroxyl and methoxy substituents on the mimic E-ring.³⁹ Importantly, we identified compound ARN16267 ($IC_{50} = 30 \pm 6 \mu M$, structure in Figure 1, which was originally named compound 3 in ref 39), which is a more potent topoII blocker than the template compounds, i.e., etoposide ($IC_{50} = 120 \pm 10 \mu M$) and merbarone ($IC_{50} = 120 \pm 12 \mu M$).³⁹ Intriguingly, we found that ARN16267 was the most efficient of this new chemical class in generating accumulation of topoII/DNA cleavage complex. This suggests that ARN16267 may act as a topoII poison, although this mechanism was less marked than that of etoposide.³⁹

These results prompted us to investigate the SAR of these new hybrid topoII blockers. Here we present an additional 16 derivatives that expand the initial panel of merbarone–etoposide hybrid molecules.³⁹ As described in Figure 1, we used ARN16267 as our best starting point for further derivatization of its core scaffold, generating scaffolds of types B and C (Figure 1). We thus identified a new hybrid derivative (3f, ARN24139; see Scheme 1) with improved human topoII inhibitory activity ($7.3 \pm 1.5 \mu M$). In addition, our results confirm that this new class of hybrid compounds acts as topoII poisons, generating accumulation of topoII/DNA cleavage complex. Our dynamic docking simulations support binding of 3f at the cleavage complex. Additionally, 3f showed high kinetic solubility and metabolic stability, as well as a promising antiproliferative activity in the low μM range against DU145, HeLa, and A549 cancer cell lines. Finally, we found 3f to have a good pharmacokinetic profile *in vivo*. Thus,

Scheme 1. Synthesis of Compounds 3a–j^a



^aOur lead compound 3f (ARN24139) is in the right column.

3f can be added to the pipeline of compounds that are active against topoII with promising anticancer activity.^{41–43}

RESULTS AND DISCUSSION

Exploring the Structure of the New Hybrid Scaffold.

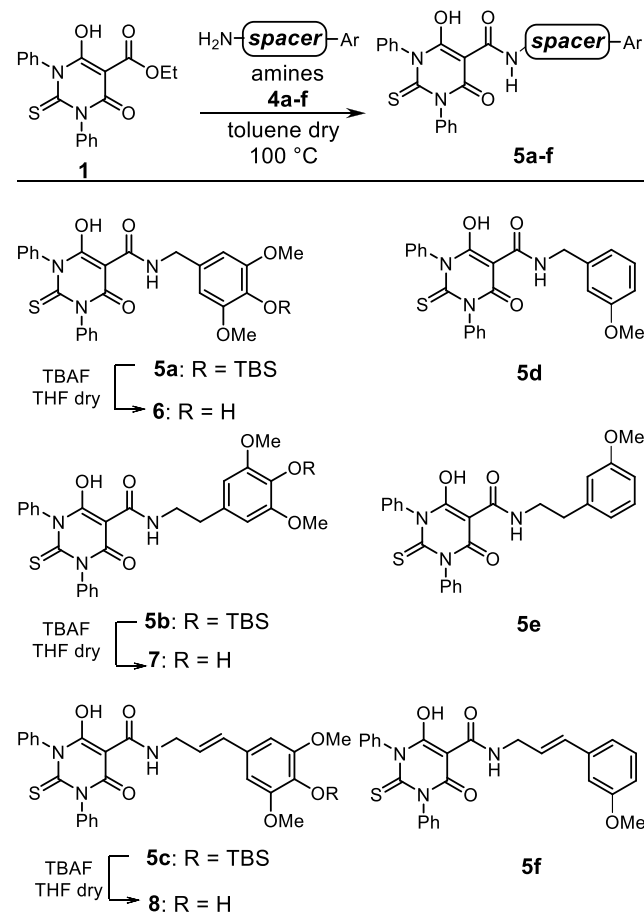
For our new set of hybrid analogues and based on our previous work and results,³⁹ we initially expanded our SAR studies by exploring the effect of diverse functional groups in the *meta* position on the mimic E-ring (3a–j, Scheme 1). First, we synthesized two new compounds with an ethoxy (3a) or isopropoxy (3b) group in the *meta* position on the mimic E-ring. We previously found that replacing the methoxy in ARN16267 with a hydroxyl group significantly decreased topoII inhibitory activity.³⁹ We thus substituted the original methoxy in ARN16267 with a cyano (3c), nitro (3d), or fluoro (3e) to modulate the electron density of the mimic E-ring. Additionally, we investigated the bioisosteric replacement of the methoxy group of ARN16267 and generated three additional new hybrid compounds, each bearing a trifluoromethoxy (3f), difluoromethoxy (3g), or difluoroethoxy (3h) group in the *meta* position on the mimic E-ring. Similarly, we synthesized a derivative with the difluoromethyl group in the *meta* position on the mimic E-aromatic ring (3i). Finally, given that a fluorine proximal to a methoxy can influence the overall electronic behavior of the aromatic ring,⁴⁴ we inserted a fluoro in the *para* position of ARN16267 to obtain 3j (Scheme 1).

In the crystal structure of the ternary topoII/DNA/etoposide complex, the drug molecule is stabilized by interactions with Asp463 and Arg487.²⁵ To favor the formation of these interactions for our hybrid compounds, we introduced a flexible spacer between the thiobarbituric core and the mimic E-ring (compounds 6–8 and 5d–f, Scheme 2).^{25,45–47} To test this hypothesis, we generated an additional set of six compounds with a link-mediated increased flexibility (6–8, 5d–f).

Chemistry. The 16 new derivatives were synthesized through regular amidation of ester 1³⁹ with amines 2a–j and 4a–f using either DMF or toluene dry as a solvent, with yields that ranged from 34% to 72% (Schemes 1 and 2). As previously described,⁴⁸ in the presence of amine 2j substituted with a fluorine in *para* and a methoxy group in *meta* position, the formylation side reaction performed by DMF was preferred over the alternative and desired reaction with ester 1.^{48,49} To circumvent this problem, the reaction was conducted in toluene dry at 100 °C, obtaining 3j with good yield (72%). The same strategy was used to synthesize 6–8 and 5d–f (Scheme 2), where different hydrocarbon chains were introduced between the amide and the aromatic ring. In particular, amines 4a–c and 4f (used to prepare 6–8 and 5f) were synthesized in two steps starting from silyl protected syringaldehyde 9 and *m*-anisaldehyde 12, respectively (Scheme 3). Compound 4a is a benzylamine featuring an aromatic ring with the same functionalization of the E ring of etoposide. This was obtained through the quantitative conversion of aldehyde 9 in the related *O*-methyl oxime 10, which was reduced into the desired amine 4a with NiCl₂ and NaBH₄ with 48% yield (Scheme 3, eq a).

The Henry reaction between protected syringaldehyde 9⁵⁰ and nitromethane in the presence of ammonium acetate gave (*E*)-nitrostyrene 11 with an excellent 90% yield. Compound 11 was then completely reduced with NiCl₂ and NaBH₄ into phenylethanamine 4b with 48% yield (Scheme 3, eq b). The Horner–Wadsworth–Emmons (HWE) reaction between

Scheme 2. Synthesis of Compounds 6–8 and 5d–f

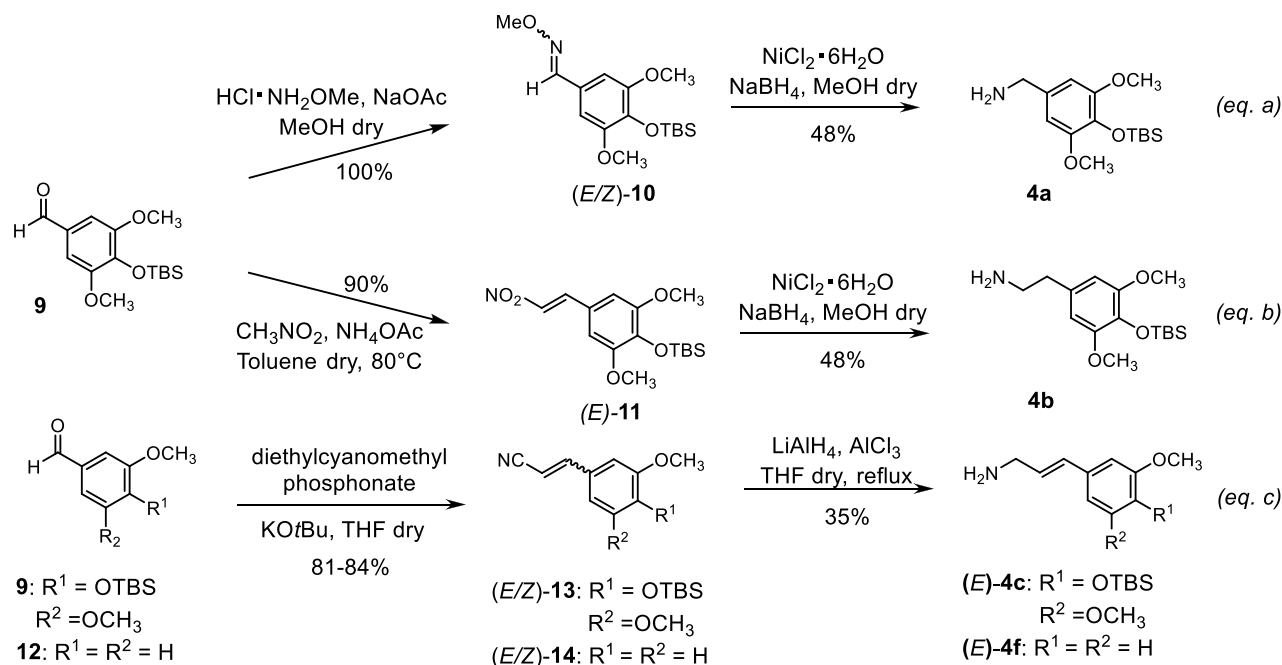


aldehyde 9⁵⁰ and diethyl cyanomethylphosphonate in the presence of potassium *tert*-butoxide in THF gave a 1:0.12 mixture of (*E*)- and (*Z*)-acrylonitrile 13 in 84% yield. The chemoselective nitrile reduction with LiAlH₄ and aluminum trichloride afforded (*E*)-allylamine 4c after chromatography purification, with an acceptable 35% yield (Scheme 3, eq c). The same sequential transformations of olefination and reduction allowed the introduction of an allylic spacer for amine 4f, starting from *m*-anisaldehyde 12, with a 22% overall yield (Scheme 3, eq c). In this case, too, the (*E*)-isomer was obtained pure after chromatography purification. Thus, the key amidation reaction between silylated amines 4a–c with ester 1 in toluene dry at 100 °C generated amides 5a–c, which were deprotected using TBAF. This yielded our final targets 6–8 with a free hydroxylic group in *para* position, with 22–38% yield after two steps (Scheme 2). Similarly, *m*-methoxyamine counterparts 5d–f were obtained with 38–62% yield using related amines 4d–f (Scheme 2).

TopoII Inhibitory Activity of the Novel Hybrid Compounds. We measured the inhibitor activity of our new compounds against human topoII α , using a topoII decatenation assay (Table 1). Notably, in our assay, etoposide returned an IC₅₀ of 47.5 ± 2.2 μ M, which agrees with the activity reported by the manufacturer of the decatenation assay kit.⁵¹ Additionally, merbarone showed an IC₅₀ of 26.0 ± 4.7 μ M, which is in line with that reported previously (IC₅₀ = 40 μ M) using a plasmid relaxation assay.³⁵

Interestingly, greater bulkiness of the alkyl chain on the oxygen in the *meta* position, as in 3a and 3b, improved the

Scheme 3. Synthesis of Amines 4a–c and 4f

Table 1. Inhibitory and Antiproliferative Activities of 16 New Derivatives 3a–j, 6–9, and 5d–f^a

compd	IC ₅₀ (μM)	DU145 (μM)	HeLa (μM)	A549 (μM)
etoposide	47.5 ± 2.2	1.0 ± 0.8	2.4 ± 0.9	1.3 ± 0.1
merbarone	26.0 ± 4.7	18.9 ± 2.0	62.3 ± 6.4	40.0 ± 2.7
ARN16267	16.1 ± 2.4	7.6 ± 0.8	5.5 ± 1.3	4.7 ± 0.3
3a	12.4 ± 3.7	5.7 ± 1.4	5.2 ± 0.9	3.6 ± 0.4
3b	9.7 ± 2.6	5.5 ± 0.1	4.2 ± 0.3	3.0 ± 0.3
3c	14.4 ± 3.8	14.4 ± 4.1	12.4 ± 1.3	16.9 ± 0.3
3d	10.2 ± 4.6	6.9 ± 0.3	11.9 ± 2.6	18.5 ± 3.1
3e	15.1 ± 4.2	5.6 ± 0.6	5.6 ± 0.5	4.1 ± 0.2
3f	7.3 ± 1.5	4.7 ± 0.1	3.8 ± 0.3	3.1 ± 0.1
3g	10.2 ± 1.9	6.5 ± 0.9	6.4 ± 0.5	4.8 ± 0.4
3h	9.2 ± 0.2	2.7 ± 2.5	2.5 ± 0.4	3.0 ± 1.1
3i	11.4 ± 2.4	7.8 ± 0.2	4.9 ± 1.4	4.4 ± 0.2
3j	22.5 ± 5.8	7.8 ± 0.6	5.3 ± 1.0	4.6 ± 0.1
5d	22.5 ± 7.2	7.7 ± 0.1	6.1 ± 1.1	4.8 ± 0.4
5e	15.8 ± 3.4	3.3 ± 2.5	3.4 ± 0.1	3.2 ± 1.2
5f	8.3 ± 2.3	5.0 ± 2.9	5.5 ± 1.1	4.4 ± 0.6
6	107.8 ± 10.1	8.8 ± 0.3	19.1 ± 4.8	14.7 ± 0.3
7	74.4 ± 13.6	13.9 ± 7.6	13.3 ± 1.7	14.8 ± 1.4
8	28.0 ± 4.4	9.8 ± 2.1	9.3 ± 0.2	9.5 ± 1.5

^aAntiproliferative activity in cancer cells of etoposide and merbarone was measured in ref 39.

potency of these compounds, as compared to ARN16267, which has an IC₅₀ of 16.1 ± 2.4 μM, as measured in the decatenation assay used in this study. In fact, 3b, with the bulkier substituent, had an IC₅₀ of 9.7 ± 2.6 μM, while the ethoxy substitution in 3a returned an IC₅₀ of 12.4 ± 3.7 μM (Table 1). We then found that the electron-withdrawing nitro group, in the *meta* position on the mimic E-ring in 3d, returned an IC₅₀ of 10.2 ± 4.6 μM. Other electron-withdrawing groups such as the cyano (3c) and the fluoro (3e) returned a comparable activity to that of ARN16267 (Table 1). This is in line with our previous demonstration of the unfavorability of

an electron-donating group, such as a hydroxyl substitution, at this position.³⁹ Similarly, introducing a fluorine proximal to the methoxy group (3j) was detrimental for activity, with an IC₅₀ of 22.5 ± 5.8 μM.

We then investigated the bioisosteric replacement of the methoxy group in *meta* position on the mimic E-ring. Interestingly, all the bioisosteric analogues 3f–h displayed a better activity than ARN16267: introducing a trifluoromethoxy group in 3f returned a 2-fold increased activity with an IC₅₀ of 7.3 ± 1.5 μM, while difluoroethyl in 3h returned an IC₅₀ of 9.2 ± 0.2 μM, and the difluoromethoxy group in 3g returned an IC₅₀ of 11.4 ± 2.4 μM. Notably, the difluoromethyl analogue 3i also had this improved activity, which confirms that the additional interactions provided by fluorinated groups (also more lipophilic) can compensate the loss of the oxy-moiety in *meta* position of the aromatic (mimic) E-ring.

After evaluating the inhibitory activity of this first subset of derivatives, we assessed the activity of the hybrid molecules with a flexible spacer connecting the thiobarbituric core and the mimic E-ring (5d–f and 6–8, Scheme 2). We started evaluating the activity of the compound 6, where we inserted a methylene substitution that contains the exact E-ring of etoposide. This first modification reduced the potency (IC₅₀ = 107.8 ± 10.1 μM), with a 7-fold drop in activity compared to ARN16267 (Table 1). Conversely, inserting the same substitution in 5d only decreased 1.4-fold the inhibitory activity (IC₅₀ = 22.5 ± 7.2 μM) compared to the parent compound ARN16267 (Table 1). This result confirms that a methoxy group, alone, in the mimic E-ring increases the potency of this hybrid scaffold, as also observed previously.³⁹ Increasing the spacer length was also beneficial, improving the IC₅₀ from over 100 μM for 6 to 74.4 ± 13.6 and 28.0 ± 4.4 μM for 7 and 8, respectively. This positive trend in potency could be due to a more balanced structure where the flexibility introduced by having the hydrocarbon chain (i.e., the spacer) is compensated by the introduced rigidity of the C=C double bond embedded in the allylic system in 8. Within this second

class of analogues, compounds are more potent when the 3-methoxy was retained as the only substituent, with IC_{50} values of $22.5 \pm 7.2 \mu\text{M}$ for **5d**, $15.8 \pm 3.4 \mu\text{M}$ for **5e**, and $8.3 \pm 2.3 \mu\text{M}$ for **5f**. Notably, **5f** showed a 2-fold increase in IC_{50} compared to its template ARN16267 (which has no spacer). These data thus suggest that a flexible substituent connecting the thiobarbituric core and the mimic E-ring in our hybrid scaffold may facilitate the orientation of our molecules inside the active site of topoII, increasing their inhibitory potency (see docking results, below).

Antiproliferative Activity against Cultured Human Cancer Cells, Metabolic Stability, Chemical Solubility, and TopoII Poisoning. The antiproliferative activity of all compounds was evaluated in (i) DU145, an androgen-independent prostate cancer cell line; (ii) HeLa, a cervical cancer cell line; and (iii) A549, a lung adenocarcinoma cell line (Table 1). Notably, all new compounds showed good antiproliferative activity with IC_{50} values in the low μM range. Among the most active compounds in inhibiting topoII activity, **3f**, **3h**, and **5e** showed cytotoxicity with IC_{50} values lower than $5 \mu\text{M}$ (Table 1). Undoubtedly, this preliminary cytotoxicity data will need further characterization, also in relation to the *in vitro* activity of these compounds.

After this initial evaluation of the new set of hybrid compounds for their inhibitory activity against topoII *in vitro* and for their biological cytotoxicity, we selected **3b**, **3f–i**, and **5e** for further evaluation. We assessed their metabolic stability using mouse serum and mouse liver microsomes, and we assessed their kinetic solubility in neutral buffer. These compounds had excellent plasma and microsomal stability with half-time values greater than 120 and 60 min, respectively. Additionally, **3f**, **3g**, and **3i** displayed excellent solubility in aqueous buffer (pH 7.4), with values greater than $200 \mu\text{M}$ (Table 2).

Table 2. Kinetic Solubility of 3b, 3f–h, 5e

compd	kinetic solubility (μM)
ARN16267	236
3b	34
3f	224
3g	208
3h	6
3i	238
5e	122

In view of these results, **3f**, **3g**, and **3i** were tested in a cleavage complex formation assay to further ascertain their mode of action as topoII poisons. As shown in Figure 2, all these hybrid molecules were confirmed to be poisons and thus able to generate an accumulation of topoII/DNA cleavage complex. In particular, **3f** had the greatest poison efficacy, being about 1.5-fold better than the template ARN16267, at $200 \mu\text{M}$ concentration. Given **3f**'s promising *in vitro* activity as a topoII poison and its overall drug-like profile, we examined its binding mode to topoII α and its *in vivo* pharmacokinetic profile in mice.

Docking and Molecular Simulations of 3f Bound to the Target. We used docking and atomistic force-field-based molecular dynamics (MD) simulations to model **3f** bound to the topoII/DNA cleavage site.^{52–55} First, the crystal structure of the topoII α isoform (PDB code 5GWK) was used for the docking studies.^{25,56} As seen in Figure S2, when the compound

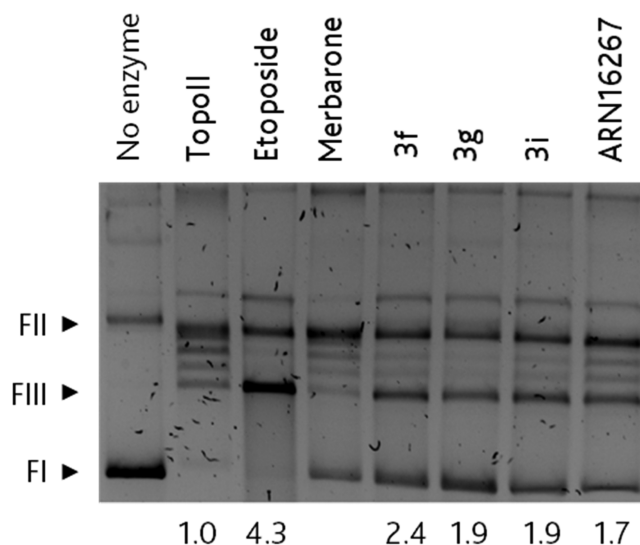


Figure 2. Poison activity of the hybrid compounds. Agarose gel electrophoresis of plasmid DNA incubated in the absence (no enzyme) or presence of 1 U of topoII containing either 1% DMSO as control vehicle (no enzyme and topoII lanes) or $200 \mu\text{M}$ compound. Labels are shown above each lane. Numbers at the bottom correspond to the normalized intensity of the linear form (FIII). Plasmid forms are indicated by the arrow-points on the right: supercoiled (FI), nicked (FII), and linear (FIII).

was first docked into the cleavage site, the mimic E-ring slightly shifted relative to the position of the E-ring of etoposide in the crystal.²⁵ Our calculations revealed several key contacts between the ligand and vicinal residues that confer the system a stable, inhibited conformation, thus endorsing the compound's action as a topoII poison. The protein aids the ligand's anchoring within the pocket by a cation– π link formed between Arg487 and the E-ring. The neighboring DNA bases also contribute to the stabilization of the complex. Specifically, the G_{+5} and C_{-1} bases display π -stacking interactions with the heterocycle inherited from merbarone (Figure 3). Similarly, the T_{+1} and C_{-1} bases align to the phenyl substituents at the thiobarbituric core in a perpendicular fashion resembling a T-shaped π -interaction. Finally, an H-bond between T_{+1} and the ligand's N–H moiety was also identified.

Once the general interaction pattern was established, we proceeded to perform equilibrium molecular dynamics (MD) simulations (~ 200 ns) to analyze the evolution and stability of the ternary topoII/DNA/**3f** model system.^{14,57–59} For this, distances representative of the interactions described above were tracked (Figure 4A). The simulations corroborate the role of Arg487 in stabilizing the drug at the cleaved site. Indeed, we monitored the distance between the carbon atom of the guanidinium group and the centroid of the E-ring and found that it remains under 6 Å for 99% of the simulation (Figure 4B).

The H-bonds between the ligand and the cleaved complex were also examined. It is worth noting that the –NH linker present in compound **3f** adds to the rigidity of the molecule. In fact, it enables the formation of a six-membered intramolecular pseudocycle. The cycled configuration was present for $\sim 79\%$ of the overall simulation time. Nonetheless, the –NH group was found to intermittently invert in order to form an H-bond with the oxygen from the deoxyribose ring of G_{+5} . The latter bond persisted for a total of $\sim 17\%$ of the production run, thus

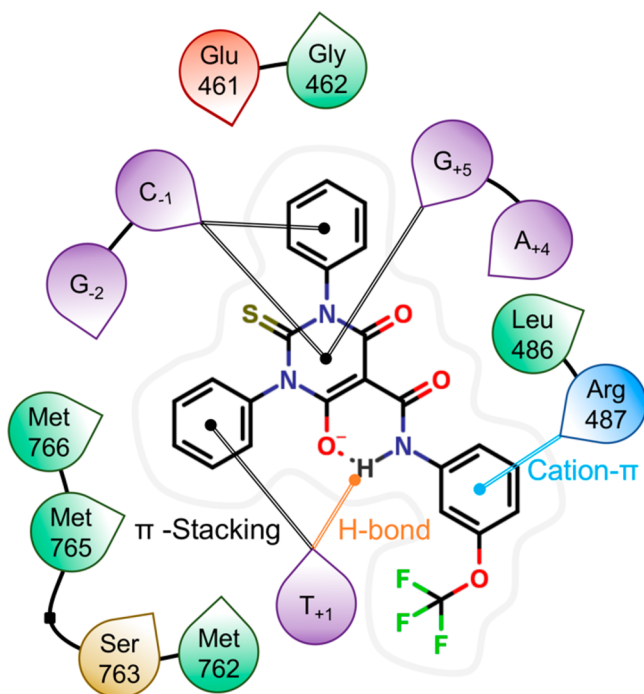


Figure 3. Interaction diagram of the lead compound **3f** bound to the DNA/topoII complex as derived from docking calculations. The computational study flags a cation- π interaction with Arg487, π -stacking with various DNA bases, and an H-bond with T₊₁, as the main drivers for ligand binding.

making a complementary interaction for the stabilization of the cleaved complex holo-form.

Similarly, we examined the staggered π -stacking formed between the thiobarbituric cycle and the G₊₅ and C₋₁ bases (Figure 4B). Here, the distance to the G₊₅ base remains consistently smaller at a stable value of 3.6 ± 0.3 Å, whereas the distance to C₋₁ extends to 4.4 ± 0.4 Å. A similar pattern is

observed between the phenyl groups and the vicinal base pairs. In summary, the binding mode most frequently visited is stable in our MD simulations too, with key cation- π , H-bonds, and stacking interactions formed with the surrounding DNA/protein complex.

In Vivo Pharmacokinetics. Finally, on the basis of the overall results and drug-like profile, **3f** was selected as our lead for *in vivo* pharmacokinetics studies, as a preparatory characterization for future analyses of *in vivo* drug efficacy in animal models of cancer. We tested two different routes of administration: (i) intravenous (iv) injection at a concentration of 3 mg/kg ($n = 3$ for each time point) and oral (po) treatment at a dose of 10 mg/kg ($n = 3$ for each time point). Despite the relatively low thermodynamic solubility of **3f** (30 μ M in PBS), the compound reached the target concentration in the formulation used for the *in vivo* experiments. The mean plasma concentration versus time profile of **3f** is shown in Figure 5, and the corresponding pharmacokinetic parameters are summarized in the inserted table. During the PK studies, via either iv or po administration, **3f** was well tolerated by all the animals, and no treatment-related clinical signs were observed.

The peak plasma **3f** concentration for iv was observed at the earliest time point (5 min after administration), and the concentration of **3f** in plasma was above the lower limit of quantification throughout the sampling period. The iv profile of **3f** presents a very fast distribution phase with a C_{max} of 7366 ng/mL, followed by a slower exposure phase. The compound was still detectable after 2 h at a concentration of 551 ng/mL, with Cl_p value of $0.004 \text{ L min}^{-1} \text{ kg}^{-1}$. After oral administration (10 mg/kg), plasma concentration of about 400 ng/mL was reached relatively quickly (1 h), and it was stably maintained for at least 6 h. The maximum concentration was achieved at approximately 2 h after oral administration, 428 ng/mL. These data indicate that the compound **3f** is well tolerated. Indeed, the animal behavior and the obtained PK profiles indicate that the dose of **3f** could be increased. This may be beneficial, given

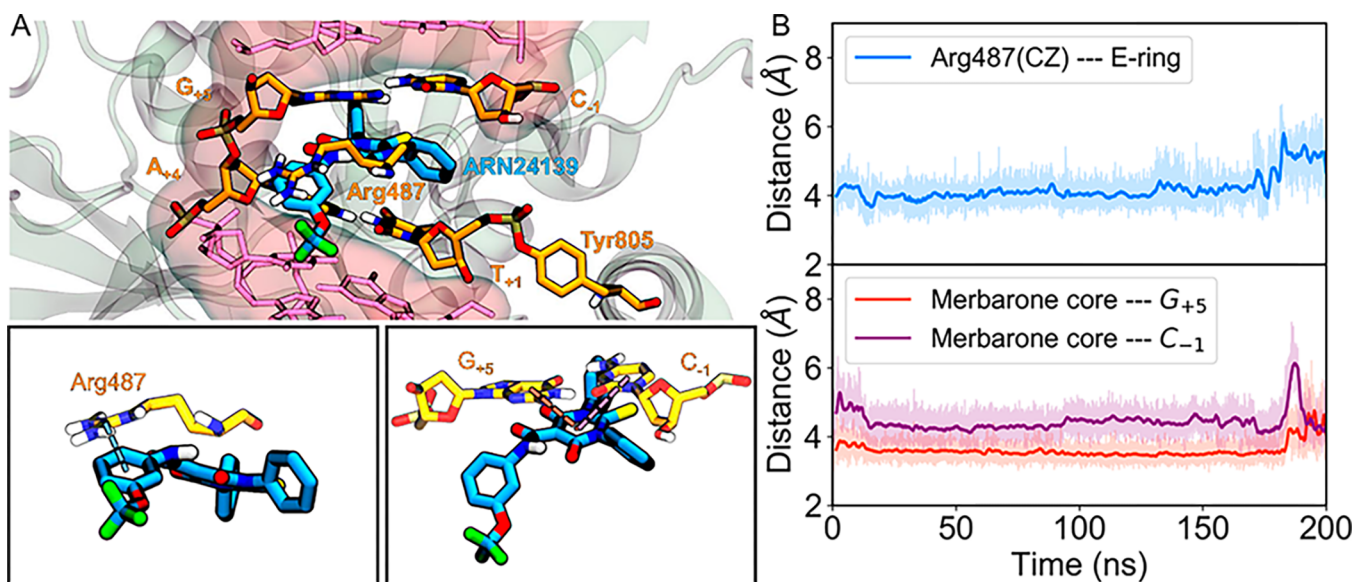


Figure 4. Dynamic description for the binding of **3f** to the in the DNA cleavage/religation active site of topoII α (PDB code 5GWK). (A) Lead compound in its binding mode. The residues directly interacting with the drug are shown in orange carbons. The rest of the DNA is shown in pink and the protein in white. The insets zoom into the distances of interest, particularly those of Arg487 with the E-ring, and the merbarone core with the G₊₅ and C₋₁ bases. (B) Evolution of the distances of interest over time.

Mouse PK Profile ARN24139

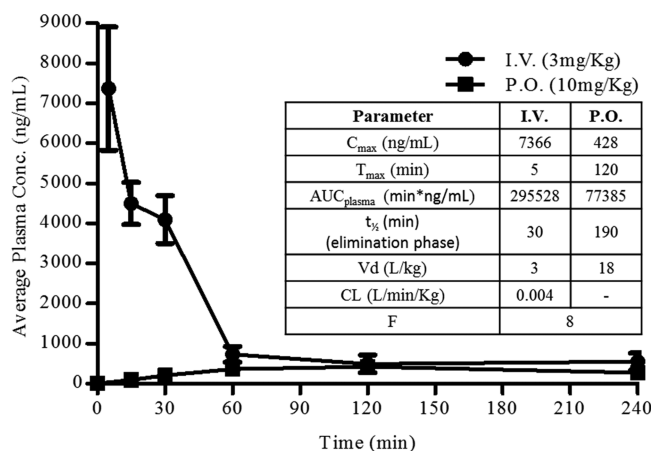


Figure 5. Mouse PK profiles of **3f** following intravenous (iv) and oral administration (po) at 3 and 10 mg/kg, respectively: observed and calculated PK parameters following intravenous (iv) and oral administration (po). The bioavailability F was calculated to 8% based on the AUC (area under curve) from $t = 0$ to 240 min.

the observed very high protein binding of this compound (>99% in both mouse and human plasma) that may limit target engagement.

CONCLUSION

On the basis of our previous results on a novel hybrid scaffold with structural elements of merbarone and etoposide,³⁹ we have here reported the design, synthesis, and extensive experimental–computational characterization of new hybrid molecules that act as topoII poisons. The resulting SAR elucidated the key structural features that enhanced the potency and antiproliferative activity of our new etoposide–merbarone hybrid compounds. These new compounds were often equipotent and sometimes more potent relative to the reference compounds merbarone and etoposide. Inhibitory activity was improved by introducing a bulkier group in *meta* position of the mimic E- ring (**3a** and **3b**, Scheme 1). Incorporating electron-withdrawing groups preserved or slightly improved the inhibitory activity (**3c–e**, Scheme 1), while the bioisosteric substitution with fluorine-embedding groups (**3f–h**, Scheme 1) was highly favorable. Furthermore, in the structural design of these new bioactive hybrid molecules, the combined functionalization of both the aromatic E-ring and the hydrocarbon spacer was essential to fine-tuning the drug–target interactions, as proven by the activity of more flexible hybrid topoII poisons (**6–8**, and **5d–f**, Scheme 2). Taken together, the inhibitory activity and extensive analyses of the drug-likeness profile indicate the novel derivative **3f** (ARN24139) as the most drug-like topoII poison of this novel chemical series. This lead compound has also shown promising antiproliferative activity against cancer cell lines and a favorable pharmacokinetic profile, which are promising features for future *in vivo* efficacy studies.

EXPERIMENTAL SECTION

Chemistry. General Considerations. All the commercially available reagents and solvents were used as purchased from vendors without further purification. Dry solvents were purchased from Sigma-Aldrich. Automated column chromatography purifications were done

using a Teledyne ISCO apparatus (CombiFlash Rf) with prepacked silica gel columns of different sizes (from 4 g up to 24 g) and mixtures of increasing polarity of cyclohexane and ethyl acetate (EtOAc) or dichloromethane (DCM) and methanol (MeOH). NMR data were collected on 400 or 600 MHz (1H) and 100 or 150 MHz (^{13}C). Spectra were acquired at 300 K, using deuterated dimethyl sulfoxide ($DMSO-d_6$) or deuterated chloroform ($CDCl_3$) as solvents. For 1H NMR, data are reported as follows: chemical shift, multiplicity (s = singlet, d = doublet, dd = double of doublets, t = triplet, q = quartet, m = multiplet), coupling constants (Hz), and integration. UPLC/MS analyses were run on a Waters ACQUITY UPLC/MS instrument consisting of an SQD (single quadrupole detector). The analyses were performed on an ACQUITY UPLC BEH C_{18} column (50×2.1 mmID, particle size $1.7 \mu m$) with a VanGuard BEH C_{18} precolumn (5×2.1 mmID, particle size $1.7 \mu m$) ($\log D > 1$). The mobile phase was 10 mM NH_4OAc in H_2O at pH 5 adjusted with AcOH (A) and 10 mM NH_4OAc in MeCN– H_2O (95:5) at pH 5 (B). Electrospray ionization in positive and negative modes was applied in the mass scan range 100–500 Da. Depending on the analysis method used, a different gradient increasing the proportion of mobile phase B was applied. For analysis method A, the mobile-phase B proportion increased from 5% to 95% in 3 min. For analysis method B, the mobile-phase B proportion increased from 50% to 100% in 3 min. High-resolution mass spectrometry (HRMS) was carried out on a Waters Synapt G2 quadrupole-Tof instrument equipped with an ESI ion source. The analyses were run on an ACQUITY UPLC BEH C_{18} column (50×2.1 mmID, particle size $1.7 \mu m$), using H_2O + 0.1% formic acid (A) and MeCN + 0.1% formic acid as mobile phase. All final compounds displayed $\geq 95\%$ purity as determined by NMR and UPLC/MS analysis.

3-(1,1-Difluoroethyl)aniline (2h). A solution of 3-nitroacetophenone (165 mg, 1 mmol) in dry CH_2Cl_2 (4 mL) was treated with [bis(2-methoxyethyl)amino]sulfur trifluoride 50 wt % solution in toluene (2.5 mmol) at room temperature under argon. EtOH (24 μL , 0.4 mmol) was added, and the reaction mixture was stirred at room temperature for 48 h, after which time, the solution was poured into $NaHCO_3$ saturated solution and extracted with CH_2Cl_2 (2×5 mL). Combined organic layers were dried with Na_2SO_4 , filtered and concentrated under vacuum. Purification by silica gel flash chromatography (elution by gradient from 100 to 95/5 cyclohexane/EtOAc) afforded pure 1-(1,1-difluoroethyl)-3-nitrobenzene (73 mg, 39% yield). 1H NMR (400 MHz, $CDCl_3$): δ 8.38 (bs, 1H), 8.31 (d, $J = 7.7$ Hz, 1H), 7.85 (d, $J = 7.7$ Hz, 1H), 7.64 (dd, $J = 7.9$, 7.9 Hz, 1H), 1.98 (t, $^3J_{H-F} = 18.2$ Hz, 3H). Then tin chloride dihydrate (440 mg, 1.95 mmol) was added to a solution of compound 1-(1,1-difluoroethyl)-3-nitrobenzene (73 mg, 0.39 mmol) in 3 mL of ethanol. The reaction mixture was refluxed for 1 h. The mixture was slowly poured on cooled water. The pH was adjusted to 7 by addition of an aqueous 5 N solution of sodium hydroxide, then adjusted to 9 by addition of an aqueous $NaHCO_3$ saturated solution. The product was extracted with EtOAc (3×5 mL). The organic phases were combined, dried over Na_2SO_4 , filtered and concentrated under vacuum. Purification by silica gel flash chromatography (elution by gradient from 100 to 80/20 cyclohexane/EtOAc) afforded pure compound **3h** (58 mg, 95% yield). UPLC/MS: Rt = 1.75 min (method A). MS (ESI) m/z : 158.0 $[M + H]^+$, $C_8H_{10}F_2N$ $[M + H]^+$ calculated, 158.1. 1H NMR (400 MHz, $CDCl_3$): δ 7.19 (dd, $J = 7.9$, 7.9 Hz, 1H), 6.89 (d, $J = 7.8$ Hz, 1H), 6.82 (bs, 1H), 6.73 (d, $J = 7.5$ Hz, 1H), bs (2H), 1.89 (t, $^3J_{H-F} = 18.2$ Hz, 3H).

General Procedure 1: Method A for Amide Formation. A solution 0.5 M ethyl 6-hydroxy-4-oxo-1,3-diphenyl-2-thioxo-1,2,3,4-tetrahydropyrimidine-5-carboxylate **1** (1 equiv) and an appropriate aniline (1 equiv) in DMF dry was stirred at 100 °C for 30 min, then cooled to room temperature, and the product was precipitated with water, filtered, and rinsed with MeOH, yielding pure compound.

General Procedure 2: Method B for Amide Formation. A solution 0.5 M ethyl 6-hydroxy-4-oxo-1,3-diphenyl-2-thioxo-1,2,3,4-tetrahydropyrimidine-5-carboxylate **1** (1 equiv) and an appropriate amine (1.2 equiv) in toluene dry was stirred at 100 °C for 2 h. After completion of reaction, the solvent was removed under vacuum. The

product was purified by flash chromatography and/or by trituration with MeOH, yielding pure compound.

***N*-(3-Ethoxyphenyl)-6-hydroxy-4-oxo-1,3-diphenyl-2-thioxo-1,2,3,4-tetrahydropyrimidine-5-carboxamide (3a).** The title compound was prepared according to general procedure 1 using 3-ethoxyaniline **2a** (31 mg, 0.23 mmol), ester **1** (86 mg, 0.23 mmol) in anhydrous DMF (0.46 mL). Then, water (3 mL) was added, and the resulting precipitate was filtered and rinsed with water (2 mL) and MeOH (2 mL), yielding **3a** (70 mg, 66% yield). UPLC/MS: Rt = 1.99 min (method A). MS (ESI) m/z : 460.4 $[M + H]^+$, $C_{25}H_{22}N_3O_4S$ $[M + H]^+$ calculated, 460.5. HRMS (AP-ESI) m/z calcd for $C_{25}H_{22}N_3O_4S$ $[M + H]^+$ 460.1331, found 460.1331. 1H NMR (400 MHz, DMSO- d_6): δ 11.63 (s, 1H, NH), 7.51–7.33 (m, 10H, Ph), 7.29 (dd, $J = 8.1, 8.1$ Hz, 1H, Ar), 7.14 (dd, $J = 2.2, 2.2$ Hz, 1H, Ar), 7.10 (dd, $J = 8.0, 1.9$ Hz, 1H, Ar), 6.80 (dd, $J = 8.2, 2.3$ Hz, 1H, Ar), 4.02 (q, $J = 7.0$ Hz, 2H), 1.30 (t, $J = 6.9$ Hz, 3H). ^{13}C (100 MHz, DMSO- d_6): δ 178.3 (CS), 168.7 (Cq), 159.0 (Cq), 139.0 (Cq), 136.4 (Cq), 130.1 (CH), 129.1 (CH), 129.0 (CH), 128.4 (CH), 114.0 (CH), 112.1 (CH), 108.1 (CH), 84.0 (Cq), 63.3 (CH₂), 14.6 (CH₃).

6-Hydroxy-*N*-(3-isopropoxyphenyl)-4-oxo-1,3-diphenyl-2-thioxo-1,2,3,4-tetrahydropyrimidine-5-carboxamide (3b). The title compound was prepared according to general procedure 1 using 3-isopropoxyaniline **2b** (45 mg, 0.30 mmol), ester **1** (110 mg, 0.30 mmol) in anhydrous DMF (0.6 mL). Then, water (3 mL) was added, and the resulting precipitate was filtered and rinsed with water (2 mL) and MeOH (2 mL), yielding **3b** (50 mg, 35% yield). UPLC/MS: Rt = 2.10 min (method A). MS (ESI) m/z : 472.4 $[M - H]^-$, $C_{26}H_{24}N_3O_4S$ $[M - H]^-$ calculated, 472.5. HRMS (AP-ESI) m/z calcd for $C_{26}H_{24}N_3O_4S$ $[M + H]^+$ 474.1488, found 474.1494. 1H NMR (400 MHz, CDCl₃): δ 11.85 (s, 1H, NH), 7.50–7.60 (m, 6H, Ph), 7.36–7.33 (m, 4H, Ph), 7.27 (dd, $J = 8.0, 5.0$ Hz, 1H, Ar), 7.08–7.04 (m, 2H, Ar), 6.79 (dd, $J = 8.3, 2.4$ Hz, 1H, Ar), 4.54 (quint, $J = 6.0$ Hz, 1H), 1.36 (d, $J = 6.0$ Hz, 6H). ^{13}C (100 MHz, CDCl₃): δ 178.6 (CS), 169.3 (Cq), 167.8 (Cq), 162.3 (Cq), 158.7 (Cq), 139.2 (Cq), 138.1 (Cq), 136.2 (Cq), 130.2 (CH), 129.8 (CH), 129.7 (CH), 129.3 (CH), 129.1 (CH), 128.8 (CH), 128.6 (CH), 114.2 (CH), 114.0 (CH), 109.5 (CH), 83.6 (Cq), 70.3 (CH), 22.1 (CH₃).

***N*-(3-Cyanophenyl)-6-hydroxy-4-oxo-1,3-diphenyl-2-thioxo-1,2,3,4-tetrahydropyrimidine-5-carboxamide (3c).** The title compound was prepared according to general procedure 1 using 3-cianoaniline **2c** (48 mg, 0.41 mmol), ester **1** (150 mg, 0.41 mmol) in anhydrous DMF (0.82 mL). Then, water (4 mL) was added, and the resulting precipitate was filtered and rinsed with water (4 mL) and MeOH (4 mL), yielding **3c** (122 mg, 68% yield) as a light pink amorphous solid. UPLC/MS: Rt = 1.75 min (method A). MS (ESI) m/z : 441.4 $[M + H]^+$, $C_{24}H_{17}N_4O_3S$ $[M + H]^+$ calculated, 441.4. HRMS (AP-ESI) m/z calcd for $C_{24}H_{17}N_4O_3S$ $[M + H]^+$ 441.1021, found 441.1025. 1H NMR (400 MHz, DMSO- d_6): δ 11.72 (s, 1H, NH), 8.10 (bs, 1H, Ar), 7.86 (d, $J = 8.2$ Hz, 1H, Ar), 7.66 (d, $J = 7.7$ Hz, Ar), 7.58 (dd, $J = 8.0, 8.0$ Hz, 1H, Ar), 7.51–7.33 (m, 10H, Ph). ^{13}C (100 MHz, DMSO- d_6): δ 178.2 (CS), 168.7 (Cq), 164.1 (Cq), 139.1 (Cq), 138.8 (Cq), 130.5 (CH), 129.1 (CH), 129.0 (CH), 128.9 (CH), 126.8 (CH), 125.1 (CH), 118.3 (Cq), 111.9 (Cq), 84.7 (Cq).

6-Hydroxy-*N*-(3-nitrophenyl)-4-oxo-1,3-diphenyl-2-thioxo-1,2,3,4-tetrahydropyrimidine-5-carboxamide (3d). The title compound was prepared according to general procedure 1 using 3-nitroaniline **2d** (38 mg, 0.27 mmol), ester **1** (100 mg, 0.27 mmol) in anhydrous DMF (0.54 mL). Then, water (4 mL) was added, and the resulting precipitate was filtered and rinsed with water (4 mL) and MeOH (4 mL), yielding **3d** (70 mg, 57% yield) as a pale yellow amorphous solid. UPLC/MS: Rt = 1.86 min (method A). MS (ESI) m/z : 461.5 $[M + H]^+$, $C_{23}H_{17}N_4O_5S$ $[M + H]^+$ calculated, 461.5. HRMS (AP-ESI) m/z calcd for $C_{23}H_{17}N_4O_5S$ $[M + H]^+$ 461.0920, found 461.0924. 1H NMR (400 MHz, DMSO- d_6): δ 11.84 (s, 1H, NH), 8.59 (dd, $J = 2.2, 2.2$ Hz, 1H, Ar), 8.01 (ddd, $J = 8.2, 2.3, 0.8$ Hz, 1H, Ar), 7.89 (ddd, $J = 8.2, 2.1, 0.8$ Hz, 1H, Ar), 7.64 (dd, $J = 8.2, 8.2$ Hz, 1H, Ar), 7.50–7.31 (m, 10H, Ph). ^{13}C NMR (100 MHz, CDCl₃): δ 178.2 (CS), 169.9 (Cq), 168.1 (Cq), 162.2 (Cq), 148.9 (Cq), 138.9 (Cq), 137.6 (Cq), 136.8 (Cq), 130.3 (CH), 129.9 (CH),

129.8 (CH), 129.6 (CH), 129.3 (CH), 128.6 (CH), 128.5 (CH), 127.0 (CH), 120.6 (CH), 116.6 (CH), 84.1 (Cq).

***N*-(3-Fluorophenyl)-6-hydroxy-4-oxo-1,3-diphenyl-2-thioxo-1,2,3,4-tetrahydropyrimidine-5-carboxamide (3e).** The title compound was prepared according to general procedure 1 using 3-fluoroaniline **2e** (48 μ L, 0.50 mmol), ester **1** (184 mg, 0.50 mmol) in anhydrous DMF (1 mL). Then, water (5 mL) was added, and the resulting precipitate was filtered and rinsed with water (5 mL) and MeOH (5 mL), yielding **3e** (82 mg, 38% yield) as a white amorphous solid. UPLC/MS: Rt = 1.86 min (method A). MS (ESI) m/z : 434.3 $[M + H]^+$, $C_{23}H_{17}FN_3O_3S$ $[M + H]^+$ calculated, 434.5. HRMS (AP-ESI) m/z calcd for $C_{23}H_{17}FN_3O_3S$ $[M + H]^+$ 434.0975, found 434.0974. 1H NMR (600 MHz, CDCl₃): δ 11.91 (s, 1H, NH), 7.59–7.56 (m, 4H, Ar), 7.53–7.49 (m, 2H, Ar), 7.41 (ddd, $J = 10.4, 2.3, 2.3$ Hz, 1H, Ar), 7.35 (m, 5H), 7.18 (dd, $J = 8.8, 2.0$ Hz, 1H, Ar), 6.94 (ddd, $J = 8.2, 8.2, 2.5$ Hz, 1H, Ar). ^{13}C NMR (150 MHz, CDCl₃): δ 178.4 (CS), 169.5 (Cq), 167.9 (Cq), 163.8 (Cq), 163.0 (d, $^1J_{CF} = 246.3$ Hz, Cq), 139.1 (Cq), 137.9 (Cq), 136.8 (d, $^3J_{CF} = 10.8$ Hz, Cq), 130.6 (d, $^3J_{CF} = 9.1$ Hz, CH), 129.9 (CH), 129.8 (CH), 129.4 (CH), 129.2 (CH), 128.7 (CH), 128.5 (CH), 117.2 (d, $^4J_{CF} = 3.0$ Hz, CH), 113.2 ($^2J_{CF} = 21.5$ Hz, CH), 109.4 (CH, $^2J_{CF} = 21.4$ Hz, CH), 83.8 (Cq). ^{19}F NMR (565 MHz): δ –110.3 (s).

6-Hydroxy-4-oxo-1,3-diphenyl-2-thioxo-*N*-(3-(trifluoromethoxy)phenyl)-1,2,3,4-tetrahydropyrimidine-5-carboxamide (3f). The title compound was prepared according to general procedure 1 using 3-trifluoromethoxyaniline **2f** (54 μ L, 0.41 mmol), ester **1** (150 mg, 0.41 mmol) in anhydrous DMF (0.82 mL). Then, water (4 mL) was added, and the resulting precipitate was filtered and rinsed with water (4 mL) and MeOH (4 mL), yielding **3f** (79 mg, 39% yield) as a white amorphous solid. UPLC/MS: Rt = 2.05 min (method A). MS (ESI) m/z : 500.3 $[M + H]^+$, $C_{24}H_{17}F_3N_3O_4S$ $[M + H]^+$ calculated, 500.5. HRMS (AP-ESI) m/z calcd for $C_{24}H_{17}F_3N_3O_4S$ $[M + H]^+$ 500.0892, found 500.0883. 1H NMR (400 MHz, DMSO- d_6): δ 11.70 (s, 1H, NH), 7.71 (s, 1H, Ar), 7.54–7.31 (m, 12H, Ar), 7.19 (d, $J = 7.7$ Hz, 1H, Ar). ^{13}C NMR (150 MHz, CDCl₃): δ 178.4 (CS), 169.6 (Cq), 168.0 (Cq), 162.2 (Cq), 149.7 (Cq), 139.0 (Cq), 137.8 (Cq), 136.8 (Cq), 130.6 (CH), 129.9 (CH), 129.8 (CH), 129.5 (CH), 129.2 (CH), 128.7 (CH), 128.5 (CH), 120.5 (q, $^1J_{CF} = 258$ Hz, Cq), 119.9 (CH), 118.4 (CH), 114.6 (CH), 83.8 (Cq). ^{19}F NMR (565 MHz): δ –57.8 (s).

***N*-(3-(Difluoromethoxy)phenyl)-6-hydroxy-4-oxo-1,3-diphenyl-2-thioxo-1,2,3,4-tetrahydropyrimidine-5-carboxamide (3g).** The title compound was prepared according to general procedure 1 using 3-(difluoromethoxy)aniline **2g** (51 μ L, 0.41 mmol), ester **1** (150 mg, 0.41 mmol) in anhydrous DMF (0.82 mL). Then, water (4 mL) was added, and the resulting precipitate was filtered and rinsed with water (4 mL) and MeOH (4 mL), yielding **3g** (67 mg, 34% yield) as a white amorphous solid. UPLC/MS: Rt = 1.95 min (method A). MS (ESI) m/z : 482.4 $[M + H]^+$, $C_{24}H_{18}F_2N_3O_3S$ $[M + H]^+$ calculated, 482.5. HRMS (AP-ESI) m/z calcd for $C_{24}H_{18}F_2N_3O_3S$ $[M + H]^+$ 482.0986, found 482.0984. 1H NMR (600 MHz, CDCl₃): δ 11.9 (s, 1H, NH), 7.58–7.50 (m, 6H, Ar), 7.38–7.31 (m, 7H), 7.00 (d, $J = 8.1$ Hz, 1H, Ar), 6.52 (t, $J = 73.4$ Hz, 1H, CHF₂). ^{13}C NMR (150 MHz, CDCl₃): δ 178.4 (CS), 169.6 (Cq), 167.9 (Cq), 162.2 (Cq), 151.6 (Cq), 139.1 (Cq), 137.9 (Cq), 136.7 (Cq), 130.6 (CH), 129.9 (CH), 129.8 (CH), 129.5 (CH), 129.2 (CH), 128.7 (CH), 128.5 (CH), 118.6 (CH), 117.1 (CH), 115.7 (t, $^1J_{CF} = 260.5$ Hz, CH), 113.3 (CH), 83.8 (Cq). ^{19}F NMR (565 MHz): δ –81.2 (s).

***N*-(3-(1,1-Difluoroethyl)phenyl)-6-hydroxy-4-oxo-1,3-diphenyl-2-thioxo-1,2,3,4-tetrahydropyrimidine-5-carboxamide (3h).** The title compound was prepared according to general procedure 1 using 3-(1,1-difluoroethyl)aniline **2h** (50 mg, 0.32 mmol), ester **1** (117 mg, 0.32 mmol) in anhydrous DMF (0.64 mL). Then, water (3 mL) was added, and the resulting precipitate was filtered and rinsed with water (3 mL) and MeOH (3 mL), yielding **3h** (104 mg, 68% yield) as a white amorphous solid. UPLC/MS: Rt = 2.08 min (method B). MS (ESI) m/z : 480.1 $[M + H]^+$, $C_{25}H_{20}F_2N_3O_3S$ $[M + H]^+$ calculated, 480.5. HRMS (AP-ESI) m/z calcd for $C_{25}H_{20}F_2N_3O_3S$ $[M + H]^+$ 480.1193, found 480.1194. 1H

NMR (400 MHz, CDCl₃): δ 11.95 (s, 1H, NH), 7.63–7.47 (m, 8H, Ar), 7.44 (dd, J = 7.9, 7.9 Hz, 1H, Ar), 7.37 (d, J = 7.9 Hz, 1H, Ar), 7.33–7.29 (m, 4H), 1.90 (t, J = 18.2 Hz, 3H). ¹³C (100 MHz, CDCl₃): δ 178.5 (CS), 169.5 (Cq), 167.9 (Cq), 162.3 (Cq), 139.7 (t, ² J_{CF} = 27.3 Hz, Cq), 139.1 (Cq), 137.9 (Cq), 135.6 (Cq), 129.9 (CH), 129.8 (CH), 129.5 (CH), 129.2 (CH), 128.7 (CH), 122.9 (CH), 122.5 (t, ³ J_{CF} = 5.9 Hz, CH), 121.3 (t, ¹ J_{CF} = 239.5 Hz, CF₂), 118.2 (t, ³ J_{CF} = 6.4 Hz, CH), 83.7 (Cq), 26.0 (t, ² J_{CF} = 29.5 Hz, CH₃). ¹⁹F NMR (565 MHz): δ -87.1 (s).

N-(3-(Difluoromethyl)phenyl)-6-hydroxy-4-oxo-1,3-diphenyl-2-thioxo-1,2,3,4-tetrahydropyrimidine-5-carboxamide (3i). The title compound was prepared according to general procedure 1 using 3-(difluoromethyl)aniline 2i (43 mg, 0.30 mmol), ester 1 (110 mg, 0.30 mmol) in anhydrous DMF (0.60 mL). Then, water (3 mL) was added, and the resulting precipitate was filtered and rinsed with water (3 mL) and MeOH (3 mL), yielding 3i (45 mg, 32% yield) as a white amorphous solid. UPLC/MS: Rt = 1.94 min (method A). MS (ESI) m/z : 466.4 [M + H]⁺, C₂₄H₁₈F₂N₃O₃S [M + H]⁺ calculated, 466.5. HRMS (AP-ESI) m/z calcd for C₂₄H₁₈F₂N₃O₃S [M + H]⁺ 466.1037, found 466.1041. ¹H NMR (600 MHz, CDCl₃): δ 11.97 (s, 1H, NH), 7.68 (s, 1H), 7.61–7.47 (m, 8H, Ar), 7.38–7.31 (m, 5H, Ar), 6.63 (t, J = 56.5 Hz, 1H, CHF₂). ¹³C (150 MHz, CDCl₃): δ 178.5 (CS), 169.6 (Cq), 167.9 (Cq), 162.2 (Cq), 139.1 (Cq), 137.9 (Cq), 135.9 (Cq), 135.8 (t, ² J_{CF} = 22.6 Hz, Cq), 130.0 (CH), 129.9 (CH), 129.8 (CH), 129.5 (CH), 129.2 (CH), 128.7 (CH), 128.5 (CH), 123.8 (CH), 123.3 (t, ³ J_{CF} = 6.1 Hz, CH), 119.0 (t, ³ J_{CF} = 6.1 Hz, CH), 119.0 (t, ³ J_{CF} = 6.2 Hz, CH), 114.0 (t, ¹ J_{CF} = 240.8 Hz, CH), 83.8 (Cq). ¹⁹F NMR (565 MHz): δ -111.5 (s).

N-(4-Fluoro-3-methylphenyl)-6-hydroxy-4-oxo-1,3-diphenyl-2-thioxo-1,2,3,4-tetrahydropyrimidine-5-carboxamide (3j). The title compound was prepared according to general procedure 2 using 4-fluoro-3-methoxyaniline 2j (61 mg, 0.43 mmol), ester 1 (132 mg, 0.36 mmol) in anhydrous toluene (0.72 mL). Then, the solvent was removed under vacuum, the residue was treated with water (3 mL), and the resulting precipitate was filtered and rinsed with MeOH (3 mL), yielding 3j (126 mg, 72% yield) as a white amorphous solid. UPLC/MS: Rt = 1.94 min (method A). MS (ESI) m/z : 464.4 [M + H]⁺, C₂₄H₁₉FN₃O₄S [M + H]⁺ calculated, 464.5. HRMS (AP-ESI) m/z calcd for C₂₄H₁₉FN₃O₄S [M + H]⁺ 464.1080, found 464.1084. ¹H NMR (600 MHz, CDCl₃): δ 11.84 (s, 1H, NH), 7.59–7.49 (m, 6H, Ar), 7.34–7.31 (m, 4H), 7.09–7.06 (m, 3H). ¹³C (150 MHz, CDCl₃): δ 178.5 (CS), 169.1 (Cq), 167.8 (Cq), 162.3 (Cq), 150.4 (¹ J_{CF} = 245.4 Hz, Cq), 148.1 (² J_{CF} = 11.3 Hz, Cq), 139.1 (Cq), 138.0 (Cq), 131.5 (d, ⁴ J_{CF} = 3.3, Cq), 129.9 (CH), 129.8 (CH), 129.4 (CH), 129.1 (CH), 128.7 (CH), 128.5 (CH), 116.5 (d, ² J_{CF} = 19.6 Hz, CH), 114.1 (d, ³ J_{CF} = 6.8 Hz, CH), 107.6 (CH), 83.6 (Cq), 56.4 (OCH₃). ¹⁹F NMR (565 MHz): δ -136.7.

[4-*tert*-Butyl(dimethyl)silyloxy-3,5-dimethoxy-phenyl]methanamine (4a). A suspension of compound 10 (250 mg, 0.77 mmol) in 7 mL of dry MeOH was cooled to 0 °C and treated with NiCl₂·6H₂O (734.0 mg, 3.09 mmol). The resulting mixture was stirred at the same temperature for 5 min before the addition of NaBH₄ (290 mg, 7.66 mmol). After 30 min, the reaction mixture was quenched with saturated aqueous NH₄Cl (10 mL) solution and extracted with EtOAc (3 × 15 mL). The combined extracts were dried over Na₂SO₄ and concentrated under vacuum. Flash chromatographic purification (elution by gradient from 100 to 80/20 DCM/MeOH·NH₃ 1 N) afforded compound 4a (110 mg, 48% yield) as a viscous oil. UPLC/MS: Rt = 0.94 min (method B). MS (ESI) m/z : 281 of main fragment. ¹H NMR (400 MHz, CDCl₃): δ 6.51 (s, 2H), 3.80 (bs, 2H), 3.79 (s, 6H), 1.00 (s, 9H, *t*Bu TBS), 0.12 (s, 6H, CH₃ TBS).

2-[4-*tert*-Butyl(dimethyl)silyloxy-3,5-dimethoxyphenyl]ethanamine (4b). A suspension of compound 11 (250 mg, 0.74 mmol) in 7 mL of dry MeOH was cooled to 0 °C and treated with NiCl₂·6H₂O (703.6 mg, 2.96 mmol). The resulting mixture was stirred at the same temperature for 5 min before the addition of NaBH₄ (279.9 mg, 7.40 mmol). After 30 min, the reaction mixture was quenched with saturated aqueous NH₄Cl (10 mL) solution and extracted with EtOAc (3 × 15 mL). The combined extracts were

dried over Na₂SO₄ and concentrated under vacuum. Flash chromatographic purification (elution by gradient from 100 to 80/20 DCM/MeOH·NH₃ 1 N) afforded compound 4b (110 mg, 48% yield) as a viscous oil. UPLC/MS: Rt = 1.16 min (method B). MS (ESI) m/z : 312.2 [M + H]⁺, C₁₆H₃₀NO₃Si [M + H]⁺ calculated, 312.2. ¹H NMR (400 MHz, DMSO-*d*₆): δ 6.45 (s, 2H), 3.75 (s, 6H), 2.75 (m, 2H), 2.55 (m, 2H), 1.00 (s, 9H, *t*Bu TBS), 0.12 (s, 6H, CH₃ TBS).

(*E*)-3-[4-*tert*-Butyl(dimethyl)silyloxy-3,5-dimethoxyphenyl]prop-2-en-1-amine (4c). A 2 M solution of LiAlH₄ in THF (1.37 mL, 2.73 mmol) was added to a suspension of AlCl₃ (363 mg, 2.73 mmol) in THF dry (6 mL) at 0 °C under argon. After 10 min, a solution of intermediate 13 (774 mg, 0.78 mmol) in 5 mL of dry THF was added dropwise. The mixture was stirred for 30 min at 50 °C and then cooled at 0 °C, quenched with ice–water (5 mL). The pH was adjusted to 9–10 with NaOH 2 M solution. The mixture was extracted with EtOAc (3 × 20 mL). The combined organic extracts were dried over Na₂SO₄ and concentrated under vacuum. The ¹H NMR of the crude of the reaction showed the presence of *E/Z* isomers in ratio 1:0.12. Flash chromatographic purification (elution by gradient from 100 to 80/20 DCM/MeOH·NH₃ 1 N) afforded compound (*E*)-4c (90 mg, 35% yield) as a viscous oil. UPLC/MS: Rt = 1.26 min (method B). MS (ESI) m/z : 307.2 main fragment. ¹H NMR (400 MHz, CDCl₃): δ 6.58 (s, 2H), 6.41 (dd, J = 16.0, 1.5 Hz, 1H), 6.20 (ddd, J = 15.8, 6.0, 6.0 Hz, 1H), 3.80 (s, 6H), 3.47 (dd, J = 6.0, 1.4 Hz, 2H), 1.00 (s, 9H, *t*Bu TBS), 0.12 (s, 6H, CH₃ TBS).

(*E*)-2-(3-Methoxyphenyl)ethanamine (4f). A 2 M solution of LiAlH₄ in THF (1.75 mL, 3.5 mmol) was added to a suspension of AlCl₃ (467 mg, 3.5 mmol) in anhydrous THF (8 mL) at 0 °C under argon. After 10 min, a solution of intermediate 14 (159 mg, 1.0 mmol) in 6 mL of anhydrous THF was added dropwise. The mixture was stirred for 30 min at 50 °C and then cooled at 0 °C, quenched with ice–water (7 mL). The pH was adjusted to 9–10 with NaOH 2 M solution. The mixture was extracted with EtOAc (3 × 20 mL). The combined organic extracts were dried over Na₂SO₄ and concentrated under vacuum. The ¹H NMR of the crude of the reaction showed the presence of *E/Z* isomers in ratio 1:0.10. Flash chromatographic purification (elution by gradient from 100 to 80/20 DCM/MeOH·NH₃ 1 N) yielded title compound (*E*)-4f (45 mg, 27% yield) as a yellow viscous oil. UPLC/MS: Rt = 1.15 min (method A). MS (ESI) m/z : 147.0 main fragment. ¹H NMR (400 MHz, CDCl₃): δ 7.22 (dd, J = 7.9, 7.9 Hz, 1H), 6.97 (d, J = 7.8 Hz, 1H), 6.91 (dd, J = 2.0, 2.0 Hz, 1H), 6.78 (dd, J = 8.1, 2.6 Hz, 1H), 6.48 (ddd, J = 15.9, 1.7, 1.7 Hz, 1H), 6.32 (ddd, J = 15.8, 5.8, 5.8 Hz, 1H), 3.81 (s, 3H), 3.49 (dd, J = 5.8, 1.3 Hz, 2H).

N-(4-*tert*-Butyl(dimethyl)silyloxy-3,5-dimethoxybenzyl)-6-hydroxy-4-oxo-1,3-diphenyl-2-thioxo-1,2,3,4-tetrahydropyrimidine-5-carboxamide (5a). The title compound was prepared according to general procedure 2 using amine 4a (80 mg, 0.27 mmol), ester 1 (83 mg, 0.22 mmol) in anhydrous toluene (0.44 mL). Then, the solvent was removed under vacuum. Flash chromatographic purification (elution by gradient from 100 to 85/15 cyclohexane/EtOAc) afforded 5a (95 mg, 70% yield) as a viscous oil. UPLC/MS: Rt = 2.08 min (method B). MS (ESI) m/z : 620.3 [M + H]⁺, C₃₂H₃₈N₃O₆SSi [M + H]⁺ calculated, 620.8. ¹H NMR (400 MHz, CDCl₃): δ 10.13 (dd, J = 5.8, 5.8 Hz, 1H, NH), 7.55–7.42 (m, 6H, Ph), 7.30–7.23 (m, 4H, Ph), 6.44 (s, 2H, Ar), 4.48 (d, J = 5.9 Hz, 2H), 3.76 (s, 6H), 1.00 (s, 9H), 0.12 (s, 6H). ¹³C NMR (100 MHz, CDCl₃): δ 179.0 (CS), 170.4 (CONH), 167.5 (Cq), 162.2 (Cq), 152.0 (Cq), 128.7 (CH), 127.8 (CH), 105.8 (CH), 83.1 (Cq), 56.0 (OCH₃), 45.0 (CH₂), 25.9 (CH₃, TBS), 18.8 (Cq, TBS), -4.5 (CH₃, TBS).

N-(4-*tert*-Butyl(dimethyl)silyloxy-3,5-dimethoxyphenethyl)-6-hydroxy-4-oxo-1,3-diphenyl-2-thioxo-1,2,3,4-tetrahydropyrimidine-5-carboxamide (5b). The title compound was prepared according to general procedure 2 using amine 4b (40 mg, 0.12 mmol), ester 1 (37 mg, 0.10 mmol) in anhydrous toluene (0.50 mL). Then, the solvent was removed under vacuum. Flash chromatographic purification (elution by gradient from 100 to 75/25 cyclohexane/EtOAc) afforded 5b (27 mg, 42% yield) as a viscous

oil. UPLC/MS: Rt = 2.38 min (method B). MS (ESI) m/z : 634.2 [M + H]⁺, C₃₃H₄₀N₃O₆SSi [M + H]⁺ calculated, 634.8. ¹H NMR (400 MHz, CDCl₃): δ 10.04 (dd, J = 5.7, 5.7 Hz, 1H, NH), 7.54–7.43 (m, 6H, Ph), 7.29–7.22 (m, 4H, Ph), 6.35 (s, 2H, Ar), 3.71 (s, 6H), 3.65 (ddd, J = 6.8, 6.8, 6.8 Hz, 2H), 2.80 (dd, J = 6.8, 6.8 Hz, 2H), 1.00 (s, 9H), 0.10 (s, 6H).

(E)-N-(3-(4-((tert-Butyldimethylsilyloxy)-3,5-dimethoxyphenyl)allyl)-6-hydroxy-4-oxo-1,3-diphenyl-2-thioxo-1,2,3,4-tetrahydropyrimidine-5-carboxamide (5c). The title compound was prepared according to general procedure 2 using amine **4c** (65 mg, 0.20 mmol), ester **1** (63 mg, 0.17 mmol) in anhydrous toluene (0.34 mL). Then, the solvent was removed under vacuum. Flash chromatographic purification (elution by gradient from 100 to 75/25 cyclohexane/EtOAc) afforded **5c** (43 mg, 39% yield) as a viscous oil. UPLC/MS: Rt = 2.30 min (method B). MS (ESI) m/z : 646.3 [M + H]⁺, C₃₄H₃₉N₃O₆SSi [M + H]⁺ calculated, 646.8. ¹H NMR (400 MHz, CDCl₃): δ 10.06 (dd, J = 5.3, 5.3 Hz, 1H, NH), 7.55–7.42 (m, 6H, Ph), 7.30–7.26 (m, 4H, Ph), 6.53 (s, 2H, Ar), 6.47 (ddd, J = 15.7, 1.4, 1.4 Hz, 1H), 6.02 (ddd, J = 15.7, 6.5, 6.5 Hz, 1H), 4.17 (ddd, J = 6.5, 6.5, 1.4 Hz, 2H), 3.79 (s, 6H), 1.00 (s, 9H), 0.12 (s, 6H). ¹³C NMR (100 MHz, CDCl₃): δ 179.0 (CS), 170.6 (CONH), 167.4 (Cq), 162.3 (Cq), 151.8 (Cq), 139.4 (Cq), 138.4 (Cq), 134.7 (CH), 129.7 (CH), 129.2 (CH), 128.9 (CH), 128.6 (CH), 103.9 (CH, 2C), 83.1 (Cq), 55.9 (OCH₃), 42.6 (CH₂), 25.9 (CH₃, TBS), 18.9 (Cq, TBS), –4.5 (CH₃, TBS).

6-Hydroxy-N-(3-methoxybenzyl)-4-oxo-1,3-diphenyl-2-thioxo-1,2,3,4-tetrahydropyrimidine-5-carboxamide (5d). The title compound was prepared according to general procedure 2 using 3-methoxybenzylamine **4d** (21 μL, 0.16 mmol), ester **1** (50 mg, 0.14 mmol) in anhydrous toluene (0.28 mL). Then, the solvent was removed under vacuum. Flash chromatographic purification (elution by gradient from 100 to 75/25 cyclohexane/EtOAc) afforded **5d** (39 mg, 62% yield) as an amorphous white solid. UPLC/MS: Rt = 2.26 min (method A). MS (ESI) m/z : 460.2 [M + H]⁺, C₂₅H₂₂N₃O₄S [M + H]⁺ calculated, 460.5. HRMS (AP-ESI) m/z calcd for C₂₅H₂₂N₃O₄S [M + H]⁺ 460.1331, found 460.1325. ¹H NMR (400 MHz, DMSO-*d*₆): δ 10.26 (dd, J = 6.0, 6.0 Hz, 1H, NH), 7.47–7.35 (m, 6H, Ar), 7.30–7.25 (m, 5H, Ar), 6.91–6.85 (m, 3H, Ar), 4.55 (d, J = 6.2 Hz, 2H), 3.73 (s, 3H). ¹³C (100 MHz, DMSO-*d*₆): δ 178.6 (CS), 169.7 (Cq), 159.4 (Cq), 139.3 (Cq), 138.8 (Cq), 129.8 (CH), 129.0 (CH), 128.2 (CH), 119.7 (CH), 113.6 (CH), 112.7 (CH), 82.8 (Cq), 55.1 (OCH₃), 43.7 (CH₂).

6-Hydroxy-N-(3-methoxyphenethyl)-4-oxo-1,3-diphenyl-2-thioxo-1,2,3,4-tetrahydropyrimidine-5-carboxamide (5e). The title compound was prepared according to general procedure 2 using 3-methoxyphenethylamine **4e** (38 μL, 0.26 mmol), ester **1** (80 mg, 0.22 mmol) in anhydrous toluene (0.44 mL). Then, the solvent was removed under vacuum. Flash chromatographic purification (elution by gradient from 100 to 75/25 cyclohexane/EtOAc) afforded **5e** (43 mg, 41% yield) as an amorphous white solid. UPLC/MS: Rt = 2.37 min (method A). MS (ESI) m/z : 474.1 [M + H]⁺, C₂₆H₂₄N₃O₄S [M + H]⁺ calculated, 474.1. HRMS (AP-ESI) m/z calcd for C₂₆H₂₄N₃O₄S [M + H]⁺ 474.1488, found 474.1489. ¹H NMR (400 MHz, CDCl₃): δ 10.03 (dd, J = 6.0, 6.0 Hz, 1H, NH), 7.54–7.43 (m, 6H, Ar), 7.29–7.20 (m, 5H, Ar), 6.79–6.72 (m, 3H, Ar), 3.76 (s, 3H), 3.67 (ddd, J = 6.9, 6.9, 6.9 Hz, 2H), 2.87 (dd, J = 7.2 Hz, 2H). ¹³C (150 MHz, CDCl₃): δ 179.0 (CS), 170.8 (Cq), 167.3 (Cq), 162.2 (Cq), 159.9 (Cq), 139.4 (Cq), 139.1 (Cq), 138.4 (Cq), 129.9 (CH), 129.6 (CH), 129.1 (CH), 128.9 (CH), 128.8 (CH), 128.7 (CH), 121.0 (CH), 114.4 (CH), 112.5 (CH), 83.0 (Cq), 55.3 (OCH₃), 41.9 (CH₂), 35.5 (CH₂).

(E)-6-Hydroxy-N-(3-(3-methoxyphenyl)allyl)-4-oxo-1,3-diphenyl-2-thioxo-1,2,3,4-tetrahydropyrimidine-5-carboxamide (5f). The title compound was prepared according to general procedure 2 using amine **4f** (45 mg, 0.28 mmol), ester **1** (85 mg, 0.23 mmol) in anhydrous toluene (0.46 mL). Then, the solvent was removed under vacuum, flash chromatographic purification (elution by gradient from 100 to 70/30 cyclohexane/EtOAc) afforded **5f** (42 mg, 38% yield) as an amorphous white solid. UPLC/MS: Rt = 2.33 min (method A). MS (ESI) m/z : 486.1 [M + H]⁺, C₂₇H₂₄N₃O₄S [M

+ H]⁺ calculated, 486.5. ¹H NMR (600 MHz, CDCl₃): δ 10.11 (dd, J = 5.5, 5.5 Hz, 1H, NH), 7.56–7.48 (m, 7H, Ar), 7.33–7.30 (m, 3H, Ar), 7.25 (dd, J = 8.0, 8.0 Hz, 1H, Ar), 6.95 (d, J = 7.7 Hz, 1H, Ar), 6.89 (dd, J = 2.0, 2.0 Hz, 1H, Ar), 6.84 (dd, J = 8.0, 2.2 Hz, 1H), 6.56 (d, J = 15.8 Hz, 1H), 6.18 (ddd, J = 15.8, 6.4, 6.4 Hz, 1H), 4.22 (ddd, J = 6.1, 6.1, 1.4 Hz, 2H), 3.83 (s, 3H). ¹³C NMR (150 MHz, CDCl₃): δ 179.0 (CS), 170.7 (CONH), 167.4 (Cq), 162.2 (Cq), 159.9 (Cq), 139.3 (Cq), 138.4 (Cq), 137.4 (Cq), 134.1 (CH), 129.8 (CH), 129.7 (CH), 129.2 (CH), 128.9 (CH), 128.8 (CH), 128.6 (CH, 2C), 122.8 (CH), 119.3 (CH), 114.0 (CH), 111.9 (CH), 83.1 (Cq), 55.4 (OCH₃), 42.5 (CH₂).

General Procedure 3: TBS Deprotection. A solution 0.5 M of silylated precursor (1 equiv) was treated with TBAF 1 M solution in THF (1.5 equiv). The reaction mixture stirred for 3 h. Then, the mixture was diluted with EtOAc, washed with water, and concentrated under vacuum. The crude material was purified by flash chromatography.

6-Hydroxy-N-(4-hydroxy-3,5-dimethoxybenzyl)-4-oxo-1,3-diphenyl-2-thioxo-1,2,3,4-tetrahydropyrimidine-5-carboxamide (6). The title compound was prepared according to general procedure 3 using intermediate **5a** (90 mg, 0.14 mmol), TBAF 1 M in THF (220 μL, 0.27 mmol) in anhydrous THF (0.28 mL). The crude was purified by silica gel flash chromatography (elution by gradient from 100 to 60/40 cyclohexane/EtOAc) to yield **6** (42 mg, 54%) as a pale yellow amorphous solid. UPLC/MS: Rt = 2.08 min (method A). MS (ESI) m/z : 504.2 [M – H][–], C₂₆H₂₂N₃O₆S [M – H][–] calculated, 504.5. HRMS (AP-ESI) m/z calcd for C₂₆H₂₂N₃O₆S [M + H]⁺ 506.1386, found 506.1373. ¹H NMR (400 MHz, DMSO-*d*₆): δ 10.18 (dd, J = 6.2, 6.2 Hz, 1H, NH), 8.37 (s, 1H, OH), 7.48–7.35 (m, 6H, Ph), 7.30–7.23 (m, 4H, Ph), 6.65 (s, 2H, Ar), 4.46 (d, J = 6.1 Hz, 2H), 3.73 (s, 6H). ¹³C (100 MHz, DMSO-*d*₆): δ 178.6 (CS), 169.4 (Cq), 150.0 (Cq), 139.2 (Cq), 135.3 (Cq), 128.9 (CH), 128.1 (CH), 126.7 (CH), 106.1 (CH), 82.8 (Cq), 56.1 (OCH₃), 43.7 (CH₂).

6-Hydroxy-N-(4-hydroxy-3,5-dimethoxyphenethyl)-4-oxo-1,3-diphenyl-2-thioxo-1,2,3,4-tetrahydropyrimidine-5-carboxamide (7). The title compound was prepared according to general procedure 3 using intermediate **5b** (26 mg, 0.04 mmol), TBAF 1 M in THF (60 μL, 0.06 mmol) in anhydrous THF (0.1 mL). The crude was purified by silica gel flash chromatography (elution by gradient from 100 to 60/40 cyclohexane/EtOAc) to yield **7** (11 mg, 53%) as a pale yellow amorphous solid. UPLC/MS: Rt = 2.11 min (method A). MS (ESI) m/z : 518.1 [M – H][–], C₂₇H₂₄N₃O₆S [M – H][–] calculated, 518.6. HRMS (AP-ESI) m/z calcd for C₂₇H₂₄N₃O₆S [M + H]⁺ 520.1542. ¹H NMR (400 MHz, CDCl₃): δ 10.07 (dd, J = 5.8, 5.8 Hz, 1H, NH), 7.55–7.42 (m, 6H, Ph), 7.29–7.22 (m, 4H, Ph), 6.40 (s, 2H, Ar), 5.41 (s, 1H, OH), 3.8 (s, 6H), 3.65 (ddd, J = 6.1, 6.1, 6.1 Hz, 2H), 2.81 (dd, J = 6.8 Hz, 6.8 Hz, 2H). ¹³C (150 MHz, CDCl₃): δ (CS), 179.0 (CS), 170.6 (CONH), 167.3 (Cq), 162.2 (Cq), 147.3 (Cq), 139.4 (Cq), 138.4 (Cq), 133.8 (Cq), 129.7 (CH), 129.6 (CH), 129.2 (CH), 128.9 (CH), 128.8 (CH), 128.6 (CH), 105.5 (CH), 83.0 (Cq), 56.4 (OCH₃), 42.2 (CH₂), 35.5 (CH₂).

(E)-6-Hydroxy-N-(3-(4-hydroxy-3,5-dimethoxyphenyl)allyl)-4-oxo-1,3-diphenyl-2-thioxo-1,2,3,4-tetrahydropyrimidine-5-carboxamide (8). The title compound was prepared according to general procedure 3 using intermediate **5c** (40 mg, 0.06 mmol), TBAF 1 M in THF (90 μL, 0.09 mmol) in anhydrous THF (0.12 mL). The crude was purified by silica gel flash chromatography (elution by gradient from 100 to 60/40 cyclohexane/EtOAc) to yield **8** (29 mg, 88%) as pale yellow amorphous solid. UPLC/MS: Rt = 2.11 min (method A). MS (ESI) m/z : 530.3 [M – H][–], C₂₈H₂₄N₃O₆S [M – H][–] calculated, 530.6. HRMS (AP-ESI) m/z calcd for C₂₈H₂₆N₃O₆S [M + H]⁺ 532.1542, found 532.1524. ¹H NMR (400 MHz, DMSO-*d*₆): δ 10.01 (dd, J = 6.2, 6.2 Hz, 1H, NH), 8.44 (s, 1H, OH), 7.47–7.28 (m, 11H, Ph, OH), 6.68 (m, 2H, Ar), 6.46 (d, J = 15.8 Hz, 1H), 6.17 (ddd, J = 15.8, 6.2, 6.2 Hz, 1H), 4.13 (dd, J = 6.0, 6.0, 1.4 Hz, 2H), 3.75 (s, 6H). ¹³C NMR (150 MHz, DMSO-*d*₆): δ 178.7 (CS), 169.6 (CONH), 148.1 (Cq), 139.4 (Cq), 135.7 (Cq), 132.7 (Cq), 129.1 (CH), 128.3 (CH), 126.7 (Cq), 121.7 (CH), 104.0 (CH), 83.2 (Cq), 58.0 (OCH₃), 41.9 (CH₂).

1-[4-*tert*-Butyl(dimethyl)silyloxy-3,5-dimethoxyphenyl]-*N*-methoxymethanimine (10). Sodium acetate (138 mg, 1.69 mmol) and *N*-methylhydroxylamine hydrochloride (141 mg, 1.69 mmol) were added to a solution of compound **9**⁵⁰ (250 mg, 0.844 mmol) in MeOH dry (5 mL) under argon. The reaction mixture was stirred at 50 °C for 5 h until completion of reaction. The solvent was removed under vacuum, the residue was suspended in water (5 mL), and the product was extracted with EtOAc (5 × 3 mL). Collected organic layers were dried with Na₂SO₄, filtered, and concentrated under vacuum affording desired product **10** as a mixture of *E/Z* isomers (260 mg, 95% yield). The product was used as such without further purification. UPLC/MS: Rt = 2.42 min (method B). MS (ESI) *m/z*: 326.2 [M + H]⁺, C₁₆H₂₇NO₃Si [M + H]⁺ calculated, 326.2. ¹H NMR (400 MHz, CDCl₃) of major isomer: δ 7.96 (s, 1H), 6.78 (s, 2H), 3.95 (s, 3H), 3.82 (s, 6H), 1.00 (s, 9H, *t*Bu TBS), 0.13 (s, 6H, CH₃ TBS).

1-[[1-(1-Dimethylethyl)dimethylsilyloxy]-2,6-dimethoxy-4-(1*E*)-2-nitroethenyl]benzene (11). Nitromethane (2.7 mL, 50.5 mmol) was carefully added to a mixture of aldehyde **9**⁵⁰ (300 mg, 1.01 mmol) and ammonium acetate (77.1 mg, 1.01 mmol) in toluene dry (10 mL) under argon. The reaction mixture was stirred for 20 h at reflux under argon. Then the reaction mixture was cooled at room temperature, quenched with water (10 mL), and extracted with EtOAc (2 × 10 mL). Collected organic layers were dried over Na₂SO₄, filtered and concentrated under vacuum. Flash chromatographic purification (elution by gradient from 100 to 95/5 cyclohexane/EtOAc) afforded compound (*E*)-**11** (308 mg, 90% yield) as an amorphous yellow solid. UPLC/MS: Rt = 2.41 min (method B). MS (ESI) *m/z*: 340.2 [M + H]⁺, C₁₆H₂₆NO₅Si [M + H]⁺ calculated, 340.1. ¹H NMR (400 MHz, CDCl₃): δ 7.93 (d, *J* = 13.5 Hz, 1H), 7.52 (d, *J* = 13.5 Hz, 1H), 6.73 (s, 2H), 3.84 (s, 6H), 1.01 (s, 9H, *t*Bu TBS), 0.15 (s, 6H, CH₃ TBS).

3-[4-*tert*-Butyl(dimethyl)silyloxy-3,5-dimethoxyphenyl]prop-2-enitrile (13). To a solution of diethylcyanomethyl phosphonate (180 μL, 1.1 mmol) in THF (8 mL) was added *t*-BuOK (125 mg, 1.1 mmol) at ice–water bath temperature with stirring for 30 min. After that, aldehyde **9**⁵⁰ (300 mg, 1.0 mmol) in THF (3 mL) was added dropwise into the above mixture at room temperature and was stirred overnight. The reaction mixture was quenched with water and extracted with EtOAc, washed with brine, dried over anhydrous Na₂SO₄, filtered and concentrated under vacuum. Flash chromatographic purification (elution by gradient from 100 to 85/15 cyclohexane/EtOAc) afforded title compound **13** (270 mg, 84% yield) as an *E/Z* mixture in ratio 1:0.12. UPLC/MS: Rt = 2.28 min (method B). MS (ESI) *m/z*: 320.2 [M + H]⁺, C₁₇H₂₆NO₃Si [M + H]⁺ calculated, 320.2. ¹H NMR (400 MHz, CDCl₃) for major isomer: δ 7.29 (d, *J* = 16.5 Hz, 1H), 6.63 (s, 2H), 5.71 (d, *J* = 16.5 Hz, 1H), 3.82 (s, 6H), 1.00 (s, 9H, *t*Bu TBS), 0.12 (s, 6H, CH₃ TBS).

3-(3-Methoxyphenyl)prop-2-enitrile (14). To a solution of diethylcyanomethyl phosphonate (523 μL, 3.2 mmol) in anhydrous THF (20 mL) was added *t*-BuOK (391 mg, 3.2 mmol) at ice–water bath temperature with stirring for 30 min. After that, to this mixture *m*-anisaldehyde **12** (400 mg, 2.94 mmol) in anhydrous THF (8 mL) was added dropwise at room temperature and was stirred overnight. The reaction mixture was quenched with water and extracted with EtOAc, washed with brine, dried over anhydrous Na₂SO₄, filtered and concentrated under vacuum. Flash chromatographic purification (elution by gradient from 100 to 85/15 cyclohexane/EtOAc) afforded title compound **14** (412 mg, 81% yield) as an *E/Z* mixture in ratio 1:0.18. UPLC/MS: Rt = 1.96 min (method A). MS (ESI) *m/z*: 160.0 [M + H]⁺, C₁₀H₁₀NO [M + H]⁺ calculated, 160.1. ¹H NMR (400 MHz, CDCl₃) for major isomer: δ 7.37 (d, *J* = 16.7 Hz, 1H), 7.31 (d, *J* = 7.9 Hz, 1H), 7.04 (d, *J* = 7.7 Hz, 1H), 6.98 (dd, *J* = 8.2, 2.6 Hz, 1H), 6.95 (m, 1H), 5.87 (d, *J* = 16.6 Hz, 1H), 3.83 (s, 3H).

Biology. Cell Viability Assay. Human cancer cell lines A549 (lung adenocarcinoma, ATCC CCL-185), DU-145 (androgen-independent prostate cancer, ATCC HTB-81), and HeLa (cervical carcinoma, ATCC CCL-2) were obtained from ATCC. Cells were routinely grown in minimal essential medium containing Eagle's salts and L-glutamine supplemented with 10% heat-inactivated FBS in a

humidified atmosphere of 5% CO₂ at 37 °C. To assess the antiproliferative activity of the compounds, cells were seeded at a density of 2500 cells/well (HeLa) or 5000 cells/well (A549, DU-145) in 96-well plates, and cell viability was measured using the MTT assay as described previously.³⁹ Values are reported as the mean ± SD of two independent experiments.

Topoisomerase II Activity Assay. The activity of topoIIα was measured using a decatenation assay (Inspiralis) following the manufacturer's instructions. Compounds were dissolved in DMSO and used at a concentration ranging from 200 to 1 μM. Final DMSO concentration in the assay was ≤1%. Reaction mixtures were incubated for 30 min at 37 °C and terminated with STEB buffer (40% (w/v) sucrose, 100 mM Tris-HCl, pH 8, 1 mM EDTA, 0.5 mg/mL bromophenol blue). Reaction products were resolved by electrophoresis in 1% agarose gels containing SYBR Safe DNA stain (Invitrogen), scanned, and quantified using the ChemiDoc system (BioRad). IC₅₀ values were obtained with GraphPad Prism software (version 5.03) using the band intensities of the dose–response gels. Values are reported as the mean ± SD of two independent experiments.

Topoisomerase II Cleavage Assay. Poison activity of the compounds was evaluated using a cleavage complex assay (Inspiralis) as described previously.⁶⁰ Compounds were tested at a fixed concentration of 200 μM in the presence of 1 U of topoisomerase II and 500 ng of pBR233 plasmid at 37 °C for 6 min. Final DMSO concentration in the assay was 1%. Reaction products were subjected to electrophoresis in a 1% agarose gel, stained with SYBR Safe DNA stain, and DNA bands were visualized and quantified as described above.

Computational Studies. Structural Model. The crystal structure of the α isoform of human topoII, cocrystallized with etoposide, was downloaded from the RCSB PDB repository, namely, PDB code 5GWK (α). ARN24319 was considered for the docking and classical molecular dynamic (MD) studies. The protein structure was processed with the Protein Preparation Wizard in the Schrödinger 2017 suite.⁶¹ The ligand's structure was generated and prepared with Ligprep for molecular docking, using the OPLS2005 force field and charges. All possible protonation and ionization states were generated at a pH of 7.4. Stereoisomers were generated with a limit of 32 stereoisomers per ligand.

Docking Calculations. The receptor grid for each target was prepared using the OPLS2005 force field. We specified the area surrounding the cocrystallized ligand (i.e., etoposide) as the receptor-binding pocket. The grid center was set to be the centroid of the bound etoposide. The cubic grid had a side length of 20 Å. For the receptor, we included aromatic hydrogen atoms as potential H-bond donors and halogens as potential acceptors. After grid preparation, ligands were first docked into the generated receptor grids using the extra precision (XP) scoring function. Flexible ligand sampling was considered in the docking procedure. All poses were subjected to postdocking minimization. The conformational degrees of freedom of the ligands were extensively explored by allowing nitrogen inversions as well as multiple ring conformations.

Classical MD Simulations. The most prevalent binding mode obtained from the docking studies was used for MD simulations with GROMACS version 5.1. All bonds were constrained using the P-LINCS algorithm, with an integration time step of 2 fs. The Verlet cutoff scheme was used with a minimum cutoff of 1.2 nm for short-range Lennard-Jones interactions and the real-space contribution to the fourth-order Ewald algorithm, which was used to compute long-range electrostatic interactions. Dispersion correction was applied to energy and pressure terms. Periodic boundary conditions were applied in all three dimensions. Each system was equilibrated in two phases, during which restraints were placed on protein and DNA heavy atoms. The first equilibration was done under an NVT ensemble for 500 ps using the *v*-rescale thermostat ($\tau_r = 0.1$ ps) to heat the systems until a temperature of 310 K. The NVT thermalization was followed by a 500 ps long NPT pressurization using the same thermostat and the Parrinello–Rahman barostat ($\tau_p = 2.0$ ps and $\kappa = 4.5 \times 10^{-4}$ bar⁻¹) to equilibrate the pressure at 1 bar. Production simulations

were carried out under an *NPT* ensemble in the absence of any restraints. A 200 ns production run was conducted for the complex. The analysis was carried out using programs within the GROMACS package and Python-based in-house scripts.

■ ASSOCIATED CONTENT

SI Supporting Information

The Supporting Information is available free of charge at <https://pubs.acs.org/doi/10.1021/acs.jmedchem.9b01760>.

Procedures for *in vitro* metabolic stability, aqueous kinetic solubility, aqueous thermodynamic solubility, plasma protein binding, animal models, pharmacokinetic studies, Figure S2, ^1H NMR, ^{13}C NMR, and ^{19}F NMR spectra, and chromatography analysis of key compounds (PDF)

Molecular formula strings and some data (CSV)

Coordinates information for structure representation (PDB)

■ AUTHOR INFORMATION

Corresponding Author

Marco De Vivo – Molecular Modeling and Drug Discovery Lab, Istituto Italiano di Tecnologia, 16163 Genova, Italy; Email: marco.devivo@iit.it

Authors

Jose M. Arencibia – Molecular Modeling and Drug Discovery Lab, Istituto Italiano di Tecnologia, 16163 Genova, Italy;

orcid.org/0000-0003-3227-931X

Nicoletta Brindani – Molecular Modeling and Drug Discovery Lab, Istituto Italiano di Tecnologia, 16163 Genova, Italy

Sebastian Franco-Ulloa – Molecular Modeling and Drug Discovery Lab, Istituto Italiano di Tecnologia, 16163 Genova, Italy; orcid.org/0000-0001-6128-0630

Michela Nigro – Molecular Modeling and Drug Discovery Lab, Istituto Italiano di Tecnologia, 16163 Genova, Italy

Jissy Akkarapattiakal Kuriappan – Molecular Modeling and Drug Discovery Lab, Istituto Italiano di Tecnologia, 16163 Genova, Italy

Giuliana Ottonello – Analytical Chemistry and *in Vivo* Pharmacology, Istituto Italiano di Tecnologia, 16163 Genova, Italy

Sine Mandrup Bertozzi – Analytical Chemistry and *in Vivo* Pharmacology, Istituto Italiano di Tecnologia, 16163 Genova, Italy

Maria Summa – Analytical Chemistry and *in Vivo* Pharmacology, Istituto Italiano di Tecnologia, 16163 Genova, Italy

Stefania Giroto – Molecular Modeling and Drug Discovery Lab, Istituto Italiano di Tecnologia, 16163 Genova, Italy

Rosalia Bertorelli – Analytical Chemistry and *in Vivo* Pharmacology, Istituto Italiano di Tecnologia, 16163 Genova, Italy

Andrea Armirotti – Analytical Chemistry and *in Vivo* Pharmacology, Istituto Italiano di Tecnologia, 16163 Genova, Italy; orcid.org/0000-0002-3766-8755

Complete contact information is available at: <https://pubs.acs.org/doi/10.1021/acs.jmedchem.9b01760>

Author Contributions

[§]J.M.A. and N.B. contributed equally.

Notes

The authors declare the following competing financial interest(s): One patent application protecting the class of compounds disclosed in this paper was filed by the following authors: Jose M. Arencibia and Marco De Vivo.

■ ACKNOWLEDGMENTS

M.D.V. thanks the Italian Association for Cancer Research (AIRC) for financial support (IG “23679”). We thank Grace Fox for her proofreading and copyediting.

■ ABBREVIATIONS USED

AcOH, acetic acid; Arg, arginine; ATP, adenosine triphosphate; AUC, area under the curve; C_{max} , maximum serum concentration; Cl_p, systemic plasma clearance; DCM, dichloromethane; DMF, *N,N*-dimethylformamide; DMSO, dimethyl sulfoxide; EDTA, ethylenediaminetetraacetic acid; EtOAc, ethyl acetate; *F*, bioavailability; HWE, Horner–Wadsworth–Emmons; MD, molecular dynamics; MeCN, acetonitrile; MeOH, methanol; *iv*, intravenous; PK, pharmacokinetics; *po*, per os; SAR, structure–activity relationship; TBAF, tetrabutylammonium fluoride; TBS, *tert*-butyldimethylsilyl; THF, tetrahydrofuran; topoII, topoisomeraseII

■ REFERENCES

- (1) Pommier, Y. Drugging Topoisomerases: Lessons and Challenges. *ACS Chem. Biol.* **2013**, *8*, 82–95.
- (2) Deweese, J. E.; Osheroff, N. The DNA Cleavage Reaction of Topoisomerase II: Wolf in Sheep’s Clothing. *Nucleic Acids Res.* **2009**, *37*, 738–748.
- (3) Deweese, J. E.; Osheroff, M. A.; Osheroff, N. DNA Topology and Topoisomerases: Teaching a “Knotty” Subject. *Biochem. Mol. Biol. Educ.* **2009**, *37*, 2–10.
- (4) Iacopetta, D.; Rosano, C.; Puoci, F.; Parisi, O. I.; Saturnino, C.; Caruso, A.; Longo, P.; Ceramella, J.; Malzert-Freon, A.; Dallemagne, P.; Rault, S.; Sinicropi, M. S. Multifaceted Properties of 1,4-Dimethylcarbazoles: Focus on Trimethoxybenzamide and Trimethoxyphenylurea Derivatives as Novel Human Topoisomerase II Inhibitors. *Eur. J. Pharm. Sci.* **2017**, *96*, 263–272.
- (5) Rosenblum, D.; Joshi, N.; Tao, W.; Karp, J. M.; Peer, D. Progress and Challenges Towards Targeted Delivery of Cancer Therapeutics. *Nat. Commun.* **2018**, *9*, 1410.
- (6) Hu, W.; Huang, X. S.; Wu, J. F.; Yang, L.; Zheng, Y. T.; Shen, Y. M.; Li, Z. Y.; Li, X. Discovery of Novel Topoisomerase II Inhibitors by Medicinal Chemistry Approaches. *J. Med. Chem.* **2018**, *61*, 8947–8980.
- (7) Pommier, Y.; Sun, Y.; Huang, S. N.; Nitiss, J. L. Roles of Eukaryotic Topoisomerases in Transcription, Replication and Genomic Stability. *Nat. Rev. Mol. Cell Biol.* **2016**, *17*, 703–721.
- (8) Nitiss, J. L. DNA Topoisomerase II and Its Growing Repertoire of Biological Functions. *Nat. Rev. Cancer* **2009**, *9*, 327–337.
- (9) Lindsey, R. H., jr.; Pendleton, M.; Ashley, R. E.; Mercer, S. L.; Deweese, J. E.; Osheroff, N. Catalytic Core of Human Topoisomerase II α : Insights into Enzyme–DNA Interactions and Drug Mechanism. *Biochemistry* **2014**, *53*, 6595–6602.
- (10) Liang, X.; Wu, Q.; Luan, S.; Yin, Z.; He, C.; Yin, L.; Zou, Y.; Yuan, Z.; Li, L.; Song, X.; He, M.; Lv, C.; Zhang, W. A Comprehensive Review of Topoisomerase Inhibitors as Anticancer Agents in the Past Decade. *Eur. J. Med. Chem.* **2019**, *171*, 129–168.
- (11) Wang, W.; Tse-Dinh, Y. C. Recent Advances in Use of Topoisomerase Inhibitors in Combination Cancer Therapy. *Curr. Top. Med. Chem.* **2019**, *19*, 730–740.
- (12) Hande, K. R. Topoisomerase II Inhibitors. *Cancer Chemother. Biol. Response Modif.* **2003**, *21*, 103–125.
- (13) Baldwin, E. L.; Osheroff, N. Etoposide, Topoisomerase II and Cancer. *Curr. Med. Chem.: Anti-Cancer Agents* **2005**, *5*, 363–372.

- (14) Palermo, G.; Minniti, E.; Greco, M. L.; Riccardi, L.; Simoni, E.; Convertino, M.; Marchetti, C.; Rosini, M.; Sissi, C.; Minarini, A.; De Vivo, M. An Optimized Polyamine Moiety Boosts the Potency of Human Type II Topoisomerase Poisons as Quantified by Comparative Analysis Centered on the Clinical Candidate F14512. *Chem. Commun. (Cambridge, U. K.)* **2015**, *51*, 14310–14313.
- (15) Bavisar, A. T.; Amrutkar, S. M.; Trivedi, N.; Chaudhary, V.; Nayak, A.; Guchhait, S. K.; Banerjee, U. C.; Bharatam, P. V.; Kundu, C. N. Switch in Site of Inhibition: A Strategy for Structure-Based Discovery of Human Topoisomerase II α Catalytic Inhibitors. *ACS Med. Chem. Lett.* **2015**, *6*, 481–485.
- (16) Kadayat, T. M.; Park, S.; Shrestha, A.; Jo, H.; Hwang, S. Y.; Katila, P.; Shrestha, R.; Nepal, M. R.; Noh, K.; Kim, S. K.; Koh, W. S.; Kim, K. S.; Jeon, Y. H.; Jeong, T. C.; Kwon, Y.; Lee, E. S. Discovery and Biological Evaluations of Halogenated 2,4-Diphenyl Indeno[1,2-B]Pyridinol Derivatives as Potent Topoisomerase II α -Targeted Chemotherapeutic Agents for Breast Cancer. *J. Med. Chem.* **2019**, *62*, 8194–8234.
- (17) Gouveia, R. G.; Ribeiro, A. G.; Segundo, M.; de Oliveira, J. F.; de Lima, M.; de Lima Souza, T. R. C.; de Almeida, S. M. V.; de Moura, R. O. Synthesis, DNA and Protein Interactions and Human Topoisomerase Inhibition of Novel Spiroacridine Derivatives. *Bioorg. Med. Chem.* **2018**, *26*, 5911–5921.
- (18) Pogorelnik, B.; Perdih, A.; Solmajer, T. Recent Developments of DNA Poisons–Human DNA Topoisomerase II α Inhibitors–as Anticancer Agents. *Curr. Pharm. Des.* **2013**, *19*, 2474–2488.
- (19) Pogorelnik, B.; Perdih, A.; Solmajer, T. Recent Advances in the Development of Catalytic Inhibitors of Human DNA Topoisomerase II α as Novel Anticancer Agents. *Curr. Med. Chem.* **2013**, *20*, 694–709.
- (20) Riddell, I. A.; Agama, K.; Park, G. Y.; Pommier, Y.; Lippard, S. J. Phenanthriplatin Acts as a Covalent Poison of Topoisomerase II Cleavage Complexes. *ACS Chem. Biol.* **2016**, *11*, 2996–3001.
- (21) Delgado, J. L.; Hsieh, C. M.; Chan, N. L.; Hiasa, H. Topoisomerases as Anticancer Targets. *Biochem. J.* **2018**, *475*, 373–398.
- (22) Froelich-Ammon, S. J.; Osheroff, N. Topoisomerase Poisons: Harnessing the Dark Side of Enzyme Mechanism. *J. Biol. Chem.* **1995**, *270*, 21429–21432.
- (23) Gibson, E. G.; King, M. M.; Mercer, S. L.; Dewese, J. E. Two-Mechanism Model for the Interaction of Etoposide Quinone with Topoisomerase II α . *Chem. Res. Toxicol.* **2016**, *29*, 1541–1548.
- (24) Bailly, C. Contemporary Challenges in the Design of Topoisomerase II Inhibitors for Cancer Chemotherapy. *Chem. Rev.* **2012**, *112*, 3611–3640.
- (25) Wu, C. C.; Li, T. K.; Farh, L.; Lin, L. Y.; Lin, T. S.; Yu, Y. J.; Yen, T. J.; Chiang, C. W.; Chan, N. L. Structural Basis of Type II Topoisomerase Inhibition by the Anticancer Drug Etoposide. *Science* **2011**, *333*, 459–462.
- (26) Wendorff, T. J.; Schmidt, B. H.; Heslop, P.; Austin, C. A.; Berger, J. M. The Structure of DNA-Bound Human Topoisomerase II α : Conformational Mechanisms for Coordinating Inter-Subunit Interactions with DNA Cleavage. *J. Mol. Biol.* **2012**, *424*, 109–124.
- (27) Cowell, I. G.; Sondka, Z.; Smith, K.; Lee, K. C.; Manville, C. M.; Sidorcuk-Lesthuruge, M.; Rance, H. A.; Padget, K.; Jackson, G. H.; Adachi, N.; Austin, C. A. Model for MLL Translocations in Therapy-Related Leukemia Involving Topoisomerase II β -Mediated DNA Strand Breaks and Gene Proximity. *Proc. Natl. Acad. Sci. U. S. A.* **2012**, *109*, 8989–8994.
- (28) Pendleton, M.; Lindsey, R. H., jr.; Felix, C. A.; Grimwade, D.; Osheroff, N. Topoisomerase II and Leukemia. *Ann. N. Y. Acad. Sci.* **2014**, *1310*, 98–110.
- (29) Azarova, A. M.; Lyu, Y. L.; Lin, C. P.; Tsai, Y. C.; Lau, J. Y.; Wang, J. C.; Liu, L. F. Roles of DNA Topoisomerase II Isozymes in Chemotherapy and Secondary Malignancies. *Proc. Natl. Acad. Sci. U. S. A.* **2007**, *104*, 11014–11019.
- (30) Cowell, I. G.; Austin, C. A. Mechanism of Generation of Therapy Related Leukemia in Response to Anti-Topoisomerase II Agents. *Int. J. Environ. Res. Public Health* **2012**, *9*, 2075–2091.
- (31) Pommier, Y.; Leo, E.; Zhang, H.; Marchand, C. DNA Topoisomerases and Their Poisoning by Anticancer and Antibacterial Drugs. *Chem. Biol.* **2010**, *17*, 421–433.
- (32) Hu, C. X.; Zuo, Z. L.; Xiong, B.; Ma, J. G.; Geng, M. Y.; Lin, L. P.; Jiang, H. L.; Ding, J. Salvicine Functions as Novel Topoisomerase II Poison by Binding to ATP Pocket. *Mol. Pharmacol.* **2006**, *70*, 1593–1601.
- (33) Walker, J. V.; Nitiss, J. L. DNA Topoisomerase II as a Target for Cancer Chemotherapy. *Cancer Invest.* **2002**, *20*, 570–589.
- (34) Dimaggio, J. J.; Warrell, R. P., Jr.; Muindi, J.; Stevens, Y. W.; Lee, S. J.; Lowenthal, D. A.; Haines, I.; Walsh, T. D.; Baltzer, L.; Yaldae, S.; Young, C. W. Phase I Clinical and Pharmacological Study of Merbarone. *Cancer Res.* **1990**, *50*, 1151–1155.
- (35) Fortune, J. M.; Osheroff, N. Merbarone Inhibits the Catalytic Activity of Human Topoisomerase II α by Blocking DNA Cleavage. *J. Biol. Chem.* **1998**, *273*, 17643–17650.
- (36) Malik, U. R.; Dutcher, J. P.; Caliendo, G.; Lasala, P.; Mitnick, R.; Wiernik, P. H. Phase II Trial of Merbarone in Patients with Malignant Brain Tumors. *Med. Oncol.* **1997**, *14*, 159–162.
- (37) Spallarossa, A.; Rotolo, C.; Sissi, C.; Marson, G.; Greco, M. L.; Ranise, A.; La Colla, P.; Busonera, B.; Loddo, R. Further SAR Studies on Bicyclic Basic Merbarone Analogues as Potent Antiproliferative Agents. *Bioorg. Med. Chem.* **2013**, *21*, 6328–6336.
- (38) Larsen, A. K.; Escargueil, A. E.; Skladanowski, A. Catalytic Topoisomerase II Inhibitors in Cancer Therapy. *Pharmacol. Ther.* **2003**, *99*, 167–181.
- (39) Ortega, J. A.; Riccardi, L.; Minniti, E.; Borgogno, M.; Arencibia, J. M.; Greco, M. L.; Minarini, A.; Sissi, C.; De Vivo, M. Pharmacophore Hybridization to Discover Novel Topoisomerase II Poisons with Promising Antiproliferative Activity. *J. Med. Chem.* **2018**, *61*, 1375–1379.
- (40) Ranise, A.; Spallarossa, A.; Schenone, S.; Bruno, O.; Bondavalli, F.; Pani, A.; Marongiu, M. E.; Mascia, V.; La Colla, P.; Loddo, R. Synthesis and Antiproliferative Activity of Basic Thioanalogues of Merbarone. *Bioorg. Med. Chem.* **2003**, *11*, 2575–2589.
- (41) Minniti, E.; Byl, J. A. W.; Riccardi, L.; Sissi, C.; Rosini, M.; De Vivo, M.; Minarini, A.; Osheroff, N. Novel Xanthone-Polyamine Conjugates as Catalytic Inhibitors of Human Topoisomerase II α . *Bioorg. Med. Chem. Lett.* **2017**, *27*, 4687–4693.
- (42) Oviatt, A. A.; Kuriappan, J. A.; Minniti, E.; Vann, K. R.; Onuorah, P.; Minarini, A.; De Vivo, M.; Osheroff, N. Polyamine-Containing Etoposide Derivatives as Poisons of Human Type II Topoisomerases: Differential Effects on Topoisomerase II α and II β . *Bioorg. Med. Chem. Lett.* **2018**, *28*, 2961–2968.
- (43) Riccardi, L.; Genna, V.; De Vivo, M. Metal–Ligand Interactions in Drug Design. *Nat. Rev. Chem.* **2018**, *2*, 100–112.
- (44) Meanwell, N. A. Synopsis of Some Recent Tactical Application of Bioisosteres in Drug Design. *J. Med. Chem.* **2011**, *54*, 2529–2591.
- (45) Tanaka, R.; Hirayama, N. Structure of Etoposide. *Anal. Sci.: X-Ray Struct. Anal. Online* **2007**, *23*, x29–x30.
- (46) Wilstermann, A. M.; Bender, R. P.; Godfrey, M.; Choi, S.; Anklin, C.; Berkowitz, D. B.; Osheroff, N.; Graves, D. E. Topoisomerase II - Drug Interaction Domains: Identification of Substituents on Etoposide That Interact with the Enzyme. *Biochemistry* **2007**, *46*, 8217–8225.
- (47) Bender, R. P.; Jablonksy, M. J.; Shadid, M.; Romaine, I.; Dunlap, N.; Anklin, C.; Graves, D. E.; Osheroff, N. Substituents on Etoposide That Interact with Human Topoisomerase II α in the Binary Enzyme-Drug Complex: Contributions to Etoposide Binding and Activity. *Biochemistry* **2008**, *47*, 4501–4509.
- (48) Ding, S.; Jiao, N. N,N-Dimethylformamide: A Multipurpose Building Block. *Angew. Chem., Int. Ed.* **2012**, *51*, 9226–9237.
- (49) Yang, D.-S.; Jeon, H.-B. Convenient N-Formylation of Amines in Dimethylformamide with Methyl Benzoate under Microwave Irradiation. *Bull. Korean Chem. Soc.* **2010**, *31*, 1424–1426.
- (50) Pettit, G. R.; Searcy, J. D.; Tan, R.; Cragg, G. M.; Melody, N.; Knight, J. C.; Chapuis, J. C. Antineoplastic Agents. 585. Isolation of *Bridelia ferruginea* Anticancer Podophyllotoxins and Synthesis of 4-

Aza-Podophyllotoxin Structural Modifications. *J. Nat. Prod.* **2016**, *79*, 507–518.

(51) Inspiralis Limited. <https://www.Inspiralis.Com/Assets/Technicaldocuments/Human-Topo-II-Alpha-Decatenation-Assay-Protocol.Pdf> (accessed Oct 9, 2019).

(52) De Vivo, M.; Cavalli, A. Recent Advances in Dynamic Docking for Drug Discovery. *Wiley Interdiscip. Rev.: Comput. Mol. Sci.* **2017**, *7*, No. e1320.

(53) Franco-Ulloa, S.; La Sala, G.; Miscione, G. P.; De Vivo, M. Novel Bacterial Topoisomerase Inhibitors Exploit Asp83 and the Intrinsic Flexibility of the DNA Gyrase Binding Site. *Int. J. Mol. Sci.* **2018**, *19*, 453.

(54) Kuriappan, J. A.; Osheroff, N.; De Vivo, M. Smoothed Potential MD Simulations for Dissociation Kinetics of Etoposide to Unravel Isoform Specificity in Targeting Human Topoisomerase II. *J. Chem. Inf. Model.* **2019**, *59*, 4007–4017.

(55) De Vivo, M.; Masetti, M.; Bottegoni, G.; Cavalli, A. Role of Molecular Dynamics and Related Methods in Drug Discovery. *J. Med. Chem.* **2016**, *59*, 4035–4061.

(56) Wang, Y. R.; Chen, S. F.; Wu, C. C.; Liao, Y. W.; Lin, T. S.; Liu, K. T.; Chen, Y. S.; Li, T. K.; Chien, T. C.; Chan, N. L. Producing Irreversible Topoisomerase II-Mediated DNA Breaks by Site-Specific Pt(II)-Methionine Coordination Chemistry. *Nucleic Acids Res.* **2017**, *45*, 10861–10871.

(57) Palermo, G.; Stenta, M.; Cavalli, A.; Dal Peraro, M.; De Vivo, M. Molecular Simulations Highlight the Role of Metals in Catalysis and Inhibition of Type II Topoisomerase. *J. Chem. Theory Comput.* **2013**, *9*, 857–862.

(58) Palermo, G.; Cavalli, A.; Klein, M. L.; Alfonso-Prieto, M.; Dal Peraro, M.; De Vivo, M. Catalytic Metal Ions and Enzymatic Processing of DNA and RNA. *Acc. Chem. Res.* **2015**, *48*, 220–228.

(59) Jacob, D. A.; Mercer, S. L.; Osheroff, N.; Deweese, J. E. Etoposide Quinone Is a Redox-Dependent Topoisomerase II Poison. *Biochemistry* **2011**, *50*, 5660–5667.

(60) Bandele, O. J.; Osheroff, N. Cleavage of Plasmid DNA by Eukaryotic Topoisomerase II. *Methods Mol. Biol.* **2009**, *582*, 39–47.

(61) Sastry, G. M.; Adzhigirey, M.; Day, T.; Annabhimoju, R.; Sherman, W. Protein and Ligand Preparation: Parameters, Protocols, and Influence on Virtual Screening Enrichments. *J. Comput.-Aided Mol. Des.* **2013**, *27*, 221–234.